MONTAN UNIVERSITÄT
WWW.UNILEOBEN.AC.AT

COMPARATIVE STUDY OF THE SEPARATION PERFORMANCE OF WIDE CONE ANGLE HYDROCYCLONES

FOR THE DEGREE OF

MASTER OF SCIENCE IN

RAW MATERIALS ENGINEERING

Composed at
Chair of Mineral Processing,
Department Mineral Resources Engineering
at Montanuniversitaet Leoben

SUBMITTED BY	ASSISTANCE BY
HÖFLECHNER LISA	UNIV.-PROF. DIPL.-ING. DR.MONT. HELMUT FLACHBERGER DIPL.-ING. DR.MONT. WOLFGANG ÖFNER

Leoben, May 2016

MONTAN UNIVERSITÄT
WWW.UNILEOBEN.AC.AT

AFFIRMATION

I declare in lieu of oath, that I wrote this thesis and performed the associated research myself, using only literature cited in this volume.

Ich erkläre an Eides statt, dass ich diese Arbeit selbständig verfasst, andere als die angegebenen Quellen und Hilfsmittel nicht benutzt und mich auch sonst keiner unerlaubten Hilfsmittel bedient habe.

Leoben, at 13th June 2016

.....

Name

MONTAN UNIVERSITÄT
WWW.UNILEOBEN.AC.AT

ACKNOWLEDGEMENTS

I would like to express my sincere gratitude to my supervisor Univ.-Prof. Dipl.Ing. Dr.mont. Helmut Flachberger for giving me the possibility to do my research abroad.

I further would like to thank Dipl.Ing Dr.mont. Roman Van Ommen from FLSmidth Krebs for giving me the great opportunity to carry out my experiments at FLSmidth Krebs in Tucson, Arizona. I was able to enrich both my scientific knowledge as well as my cultural experience.

A special thank you goes to my supervisor Dipl.Ing Dr.mont. Wolfgang Öfner for his guidance and advices.

In addition I thank the team of FLSmidth Krebs in Tucson. Especially I would like to thank Tim Stewart who helped me handling the machines and finishing my tests as well as Barry Buttler for his support.

Last but not least I want to thank my parents who enabled me the study and supported me throughout all this years.

MONTAN UNIVERSITÄT
WWW.UNILEOBEN.AC.AT

ABSTRACT

Hydrocyclones are used in various duties in mineral processing plants as well as in oil, recycling or chemical industries. Due to its broad areas of application, different designs are established to meet particular requirements.

In this thesis the focus is on two special types of hydrocyclones, namely water-only cyclone (WOC) and flat bottom cyclone. These types are characterized by their wide cone angle. Tests were made in the hydrocyclone lab of FLSmidth Krebs in Tucson, Arizona, with the WOC, the flat bottom and a standard hydrocyclone. The separation performance of each test is presented by use of a partition curve. Design and operational parameters were changed for each device and as a consequence thereof the separation performance observed and compared. The parameters examined were the vortex finder diameter, the vortex finder length, the type of apex installation, the apex diameter and the pressure drop. Additionally, the Krebs prognosis model was applied on the standard hydrocyclone to compare the prognosticated cut size at partition number 50% with the measured one.

MONTAN UNIVERSITÄT
WWW.UNILEOBEN.AC.AT

KURZFASSUNG

Hydrozyklone finden ihre Anwendung in verschiedenen Aufgaben in Rohstoffaufbereitungsanlagen, aber auch in anderen Industrien wie zum Beispiel der Öl-, der Recycling- oder der chemischen Industrie. Aufgrund der breiten Anwendungsgebiete haben sich verschiedene Designs für verschiedene Anforderungen entwickelt.

In dieser Arbeit liegt der Fokus auf zwei Spezialtypen des Hydrozyklons. Es handelt sich dabei um den Water-Only Cyclone (WOC) und den Flat Bottom, welche sich durch einen weiten Konuswinkel auszeichnen. Im Hydrozyklonlabor von FLSmidth Krebs in Tucson, Arizona, wurden Versuche mit dem WOC, dem Flat Bottom Zyklon und einem Standardzyklon durchgeführt. Die Güte der Trennung wurde mit Hilfe der Teilungskurve dargestellt. Für jeden Zyklon wurden Design und betriebliche Parameter verändert und die Auswirkung auf die Trenngüte beobachtet und verglichen. Die untersuchten Parameter sind Tauchrohrdurchmesser und -länge des Zyklonüberlaufs, Einbaurichtung und Durchmesser der Unterlaufdüse und das Druckgefälle. Zusätzlich wurde noch das von Krebs entwickelte Prognosemodell auf den Standardzyklon angewendet, um den prognostizierten mit dem gemessenen Trennschnitt bei einer Teilungszahl von 50% zu vergleichen.

CONTENT

1. INTRODUCTION AND OBJECTIVE

The hydrocyclone is one of the most important devices in the mineral industry. Furthermore, the hydrocyclone is applicable in the chemical industry, recycling industry or oil industry. There, the applications reach from degritting sewage sludge to removing oil droplets from produced water.[1] In mineral processing its main use is as a classifier. It is utilizing centrifugal forces for separation of particles with different terminal settling velocities. The simplicity of the device itself has many advantages. Especially for industrial use, advantages like easy handling, compactness, no moving parts, relatively low capital and operating costs, high capacity and simple maintenance are attractive. It is mostly installed in closed grinding circuits. Since comminution is not only mostly the first step in a process but also one of the most expensive ones, the importance of an efficient downstream classifier is highlighted.

Due to its broad areas of application, different designs to meet particular requirements were established. In this thesis a flat bottom and a water-only hydrocyclone were investigated. These types of hydrocyclones are characterized by their wide cone angle. The water-only cyclone with a 90° angle and the flat bottom with a 180° angle are used for very coarse separation requirements. The thesis shall help to get a better understanding of the named special types of cyclones as well as the effects on separation by changing different design and operational parameters on those.

For this purpose a test matrix with three types of hydrocyclones including a standard 20° cone, a flat bottom and a water-only hydrocyclone was developed and realized. For each device parameters were changed, observed and compared. The parameters examined were:

- Vortex finder diameter
- Vortex finder length
- Apex installation
- Apex diameter
- Pressure drop

Additionally, the Krebs prognosis model was applied for the standard hydrocyclone to compare the prognosticated D50, the D50 is the particle size where 50% of the particles present in the feed report to the underflow, with the measured one.

2. THEORY

2.1. CLASSIFICATION

The separation characteristic of classification is the terminal settling velocity. The terminal settling velocity of a solid in a fluid can be calculated from the equilibrium of forces of resistance, buoyancy and gravity.

$$\boldsymbol{F_{resistance} = F_{gravity} - F_{buoyancy}} \tag{2.1}$$

The equilibrium of forces is formulated for the motion of a spherical particle. Depending on the flow condition, friction force is based on the Stokes Law or the Newton Law. This emerge three different flow areas including a transition area. The laminar area based on Stokes, the turbulent area based on Newton and the transition area, are defined by the Reynolds number. The Reynolds number Re is a dimensionless index defined by the ratio of the variable components of inertial force $F_{inertial}$ to frictional resistance $F_{resistance}$.[2]

$$\boldsymbol{Re = \frac{var(F_{inertial})}{var(F_{resistance})}} \tag{2.2}$$

In further consequence it is represented as follows:

$$\boldsymbol{Re = \frac{d * v_s * \rho_s}{\eta}} \tag{2.3}$$

The approach for laminar flow based on Stokes is valid for Reynolds numbers below 10, based on Newton it is valid for Reynolds numbers above 1000. In between is the transition area. For laminar flow conditions, the terminal settling velocity results in:

$$\boldsymbol{v_s = \frac{d^2 * g * (\rho_s - \rho_L)}{18 * \eta}} \tag{2.4}$$

In case of a hydrocyclone, the cyclone body generates circular velocity. The centrifugal force is utilized to accelerate the settling velocity of the particles. Thus separation occurs a lot quicker. Despite turbulent flow conditions exist in a hydrocyclone, evaluations and principles are commonly described with Stokes approach. Stokes approach describes most variables affecting cyclone performance like particle size, density difference between liquid and solids and slurry viscosity.

2.2. HYDROCYCLONE

A conventional hydrocyclone consists of an upper cylindrical section and a lower conical section. The cylindrical section includes the tangential feed inlet and the vortex finder (see Figure 1). The area of the inlet nozzle at the point of entrance into the feed chamber is usually a rectangular orifice. The vortex finder functions as exit for the slurry on the top of the cylindrical section. The lower cone section includes the opening at the bottom named apex.

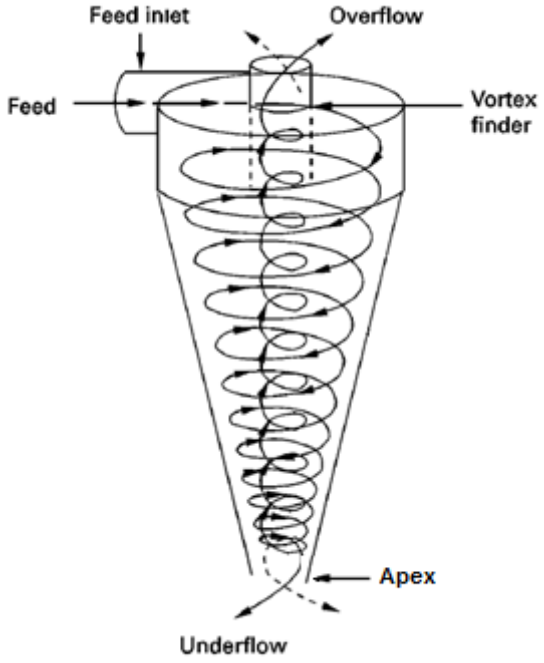

Figure 1: Schematic principle of the hydrocyclone [3]

Slurry is fed under pressure through the tangential feed inlet. The resulting swirl on the outer side of the hydrocyclone moves towards and leaves trough the apex. The built swirl in the inner side of the hydrocyclone moves upwards and leaves trough the vortex finder (see Figure 1). If one or both of the outlets are open to the atmosphere, an air core along the vertical axis inside the inner vortex stream is formed by a low pressure zone.[3]

The particles in the slurry are subjected to two counteracting forces: The centrifugal force which tends to bring the particles toward the outer wall of the hydrocyclone and the resistance force which tends to bring the particles towards the center (see Figure 2). The resistance force F_R based on Stokes and the centrifugal force F_c are represented as follows:

$$\boldsymbol{F_R = 3 * \pi * \eta * d * v_s} \tag{2.5}$$

$$F_C = (m_s - m_l) * \frac{v_s^2}{r} = \frac{\pi}{6} * d^3 * (\rho_s - \rho_l) * \frac{v_s^2}{r} \quad (2.6)$$

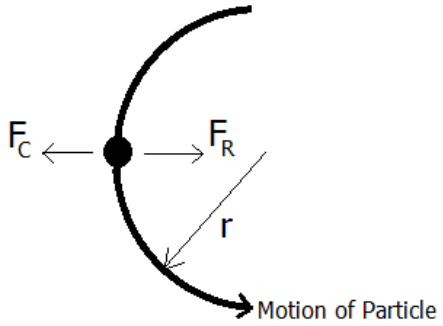

Figure 2: Forces acting on an orbiting particle

So the higher mass particles which are forced to the outer rotational path adjacent on the wall, spiral toward the bottom exiting through the apex. The lower mass particles which are more affected by the resistance forces, spiral upwards exiting through the vortex finder.

To describe the stream of the hydrocyclone it is necessary to disassemble the swirl, which is symmetrical three-dimensional around the axis of the hydrocyclone, into three components. Hence, the stream is divided in the tangential velocity, the axial velocity and the radial velocity. The tangential velocity is many times larger than the axial or radial velocity.[2] It is the component which generates the centrifugal force. The tangential velocity increases toward the air core and reaches near it a maximum and subsequently decreases steep. The axial velocity is negative near the wall and positive close to the air core. That concludes a position where the axial velocity is zero between the two vortices. The interactions between these vortices result in multiple flow reversals. By getting near the apex, the axial velocity is increasing. Figure 3 shows a qualitative image of the tangential and axial velocity distributions depending on the radius for low solid concentrations. The data refer to experiments measured by Kelsall in 1952.[4] More recent experiments using the laser Doppler velocimetry show similar results. The radial velocity is orientated towards the center of the hydrocyclone. It increases in the direction to the apex.[3]

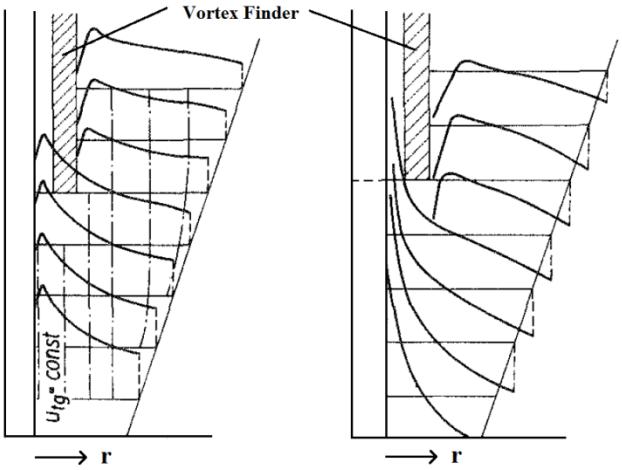

Figure 3: Qualitative image of the tangential (left) and axial velocity distributions (right) depending on the radius for low solids concentrations [2]

As experimental work has shown, the classification does not take place over the whole hydrocyclone. The profile of the hydrocyclone can be divided in four parts as seen in Figure 4. At part D the classification takes place. Unclassified feed exists at the inlet area A. At the C part the classified fines are detected. Region B is occupied by the classified coarse material.[5]

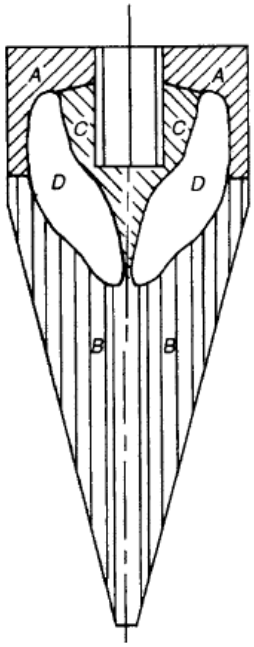

Figure 4: Areas of similar size distribution [5]

2.3. SPECIAL TYPES OF HYDROCYCLONES

2.3.1. WATER-ONLY CYCLONE

The water-only cyclone (WOC) has a short body. This type of cyclone is especially used for coal separation. Cone sections with wide cone angles as with the WOC as well as with the flat bottom allow a refuse bed to form. This refuse bed is in a circulating motion as a vertical downward flow at the wall and an upward convective flow in the center of the bed.[6] In Figure 5 the principle of the circulating motion is shown using the example of a water-only cyclone. This bed supports hindered settling conditions. Furthermore, through accumulation of the high density and coarse particles a heavy media in the second cylinder section is built. Low density particles remain on the top of the bed and are vacuumed up into the overflow by a relatively long vortex finder while heavier particles penetrate the bed and are discharged trough the apex.[7, 8]

Water-only cyclones are normally used in two stages due to coal losses in the first stage. Larger coal particles are classified trough the apex, which circumstance is eliminated in the second stage. Another application is found in the plastics industry to separate different sorts of polymers like the low density polypropylene and polyethylene particles from the high density acrylonitrile butadiene styrene (ABS) particles.[7]

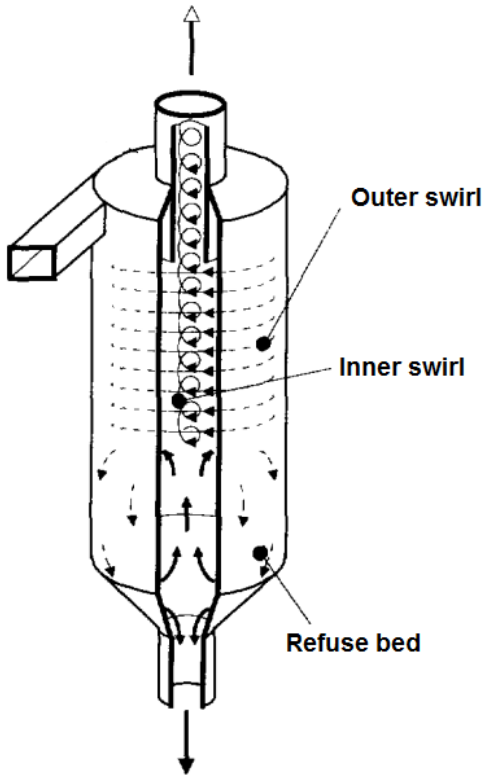

Figure 5: Principle of refuse bed in WOC [6]

2.3.2. FLAT BOTTOM

The coarsest separation is achieved by a flat bottom hydrocyclone, where the cone angle amounts to 180°. The D50 is two to three times larger in comparison with the D50 of a hydrocyclone with a 20° cone. It uses the same principle by building a refuse bed as the WOC (see Figure 5). The circumstance of the refuse bed supports the density separation of the lighter coal particles from the heavier gangue particles.[8]

Flat bottom cyclones are mostly used in closed circuit grinding systems in low-grade ore operations. Compared to conventional vertically mounted cyclones, they coarsen the separation, reduce the quantity of bypass fines and increase throughput. The reason for the decreasing amount of bypass fines is explained by the need of additional dilution water for coarser separation which results in lower feed pulp density and hence decreases the amount of bypass fines in the underflow. Flat bottom cyclones generate consistently high density underflow whereby apex diameter is not as critical as in conventional cyclones. A disadvantage is the high wear at the section where the refuse bed is circulating. Additionally, flat bottom cyclones have a flatter partition curve compared to conventional vertically mounted cyclones.[9]

2.4. VARIABLES AFFECTING HYDROCYCLONE PERFORMANCE

Since some terms are often differently interpreted it shall be mentioned that in this thesis the term "solids content" is always based on the mass and expressed in w% while the term "solids concentration" is always based on the volume and expressed in vol%.

2.4.1. DESIGN VARIABLES

Hydrocyclones have many different applications and therefore different designs are needed. The design variables described are the diameter of the hydrocyclone, the inlet design, the vortex finder, the cylinder section, the cone section, the apex, and the mounting angle.

The most obvious design variable is the diameter of the hydrocyclone. As diameter denoted is the inner diameter of the cylindrical section. The bigger the diameter the weaker appear the centrifugal forces on the particles. The relation of the diameter to the D50 is given in Figure 6.

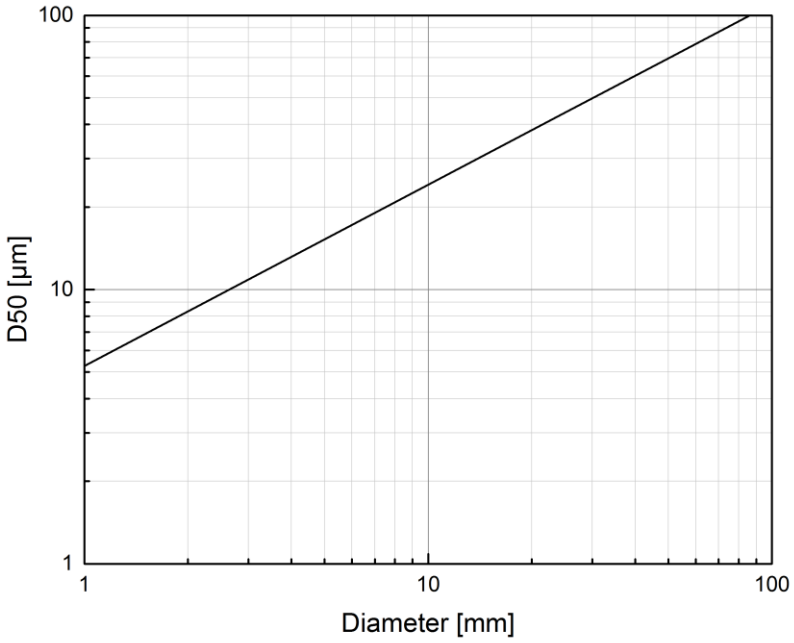

Figure 6: Relation between diameter of the hydrocyclone and the D50 [7]

On the basis of misplaced particles in the overflow due to turbulences in the inlet head, a lot of research has been done to optimize the geometry of the inlet head. Figure 7 illustrates some designs of feed entries. The latest designed entrance nozzle is the gMAX design by Krebs. Due to the involute entrance nozzle the particles already accelerate in the nozzle. Unlike a tangential feed nozzle that introduces some particles near the axis of the hydrocyclone, the gMAX design introduces the particles as a narrow ribbon near the wall. This leads to finer (i.e. lower D50) and sharper separation. A further advantage is the lower wear at the new design. It eliminates the hot spots and distributes a lower level of wear as seen in Figure 8.[7] The inlet area of the orifice on the end of the nozzle is mostly rectangular as it reduces turbulences.[10]

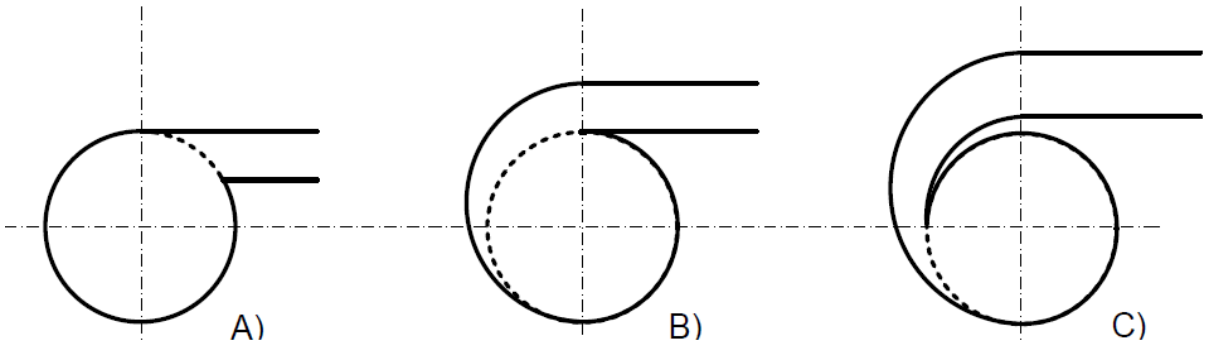

Figure 7: Different inlet designs; A) tangential inlet B) ramped inlet C) ramped involute inlet

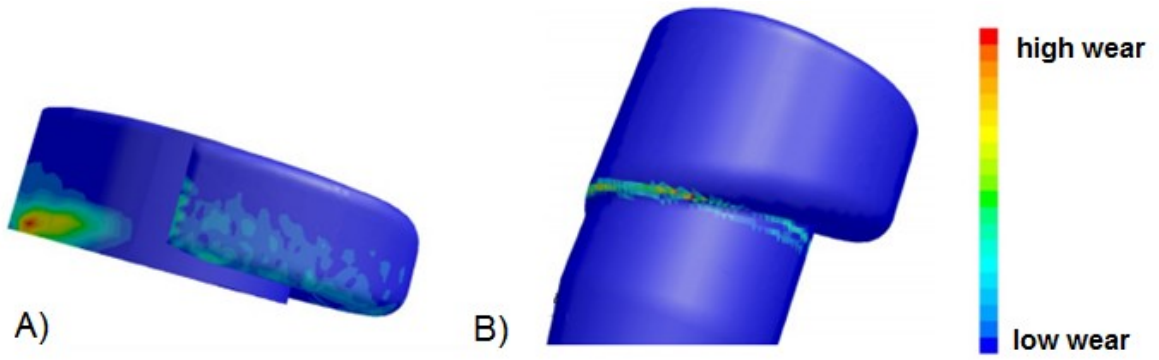

Figure 8: CFD erosion of A) old inlet design and B) new gMAX inlet design [7]

The vortex finder (VF) attempts to avoid that particles pass directly from the feed inlet to the overflow stream. The D50 decreases with the decrease of the VF diameter. This results from the decreasing radial acceleration with the increase of vortex finder diameter and the decrease of the tangential velocity according to:[11]

$$a_r = v_t^2 / r_{Vortex} \tag{2.7}$$

In Figure 9 the tangential velocity distribution is shown by computational fluid dynamics (CFD) simulation.

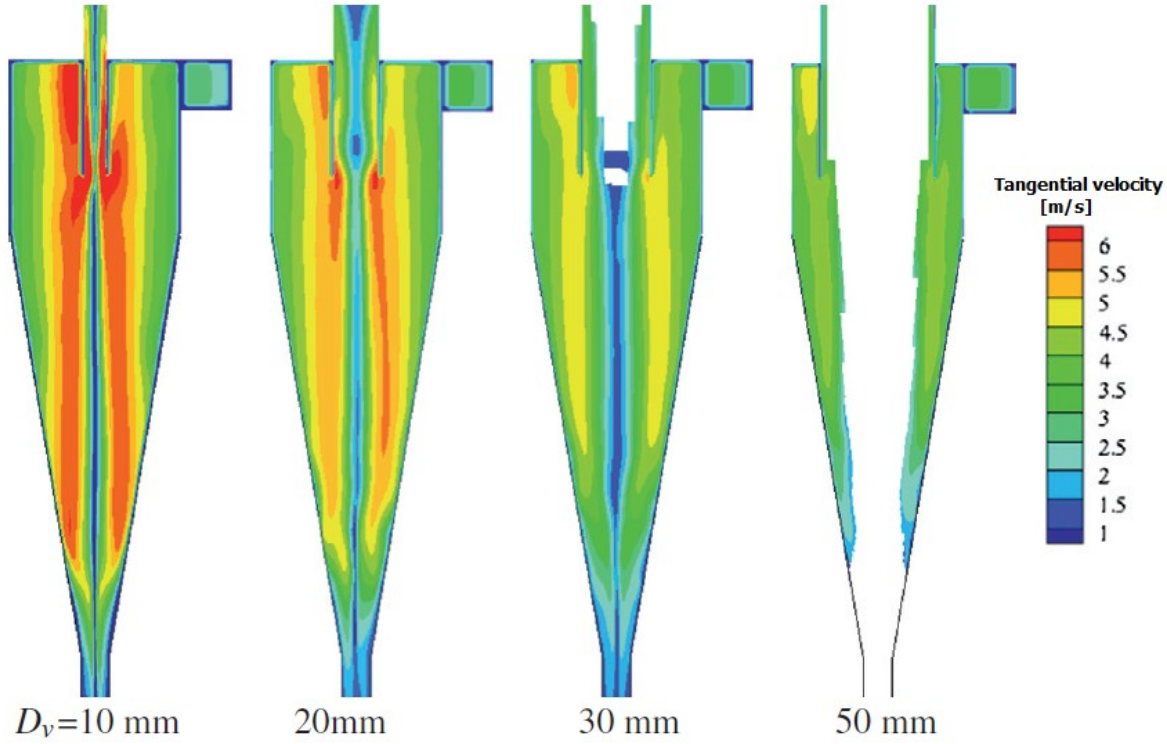

Figure 9: Tangential velocity distribution for different VF diameters (D_v) at a solids concentration of 30 vol% [11]

However, if the diameter is too small, the upward flow may not be developed at the lower part of the hydrocyclone. This is because of the large tangential velocities in this area caused by the powerful swirling flow. On the other hand, for high solids concentration it is obtained that the tangential velocities in this area decreases because of the accumulation of particles.[11] For conventional designs the vortex finder diameter is 0.35 times the hydrocyclone diameter.[10]

Also the change of the vortex finder length influences separation performance, whereby the influence is not as big as the influence of the diameter. The vortex finder length is the distance from the tip of the vortex finder to the roof of the hydrocyclone. Numerical analyses have shown that in low feed solids concentration the D50 is getting slightly coarser by increasing the VF length. This is explained by large tangential velocities which are beneath the tip of the vortex finder wall and stay near the air core until the lower part of the cone section. Through increasing the vortex finder length this space where normally the tangential velocity increases is decreased. In high feed solids concentration the D50 decreases with increasing vortex finder length. The separation region with large tangential velocities takes place gradually more in the middle between air core and wall of the hydrocyclone and not anymore at the tip of the VF by increasing the VF length. This behavior is shown by CFD simulation in Figure 10.[11] For conventional designs the vortex finder length is approximately 0.55 times the hydrocyclone diameter.[10]

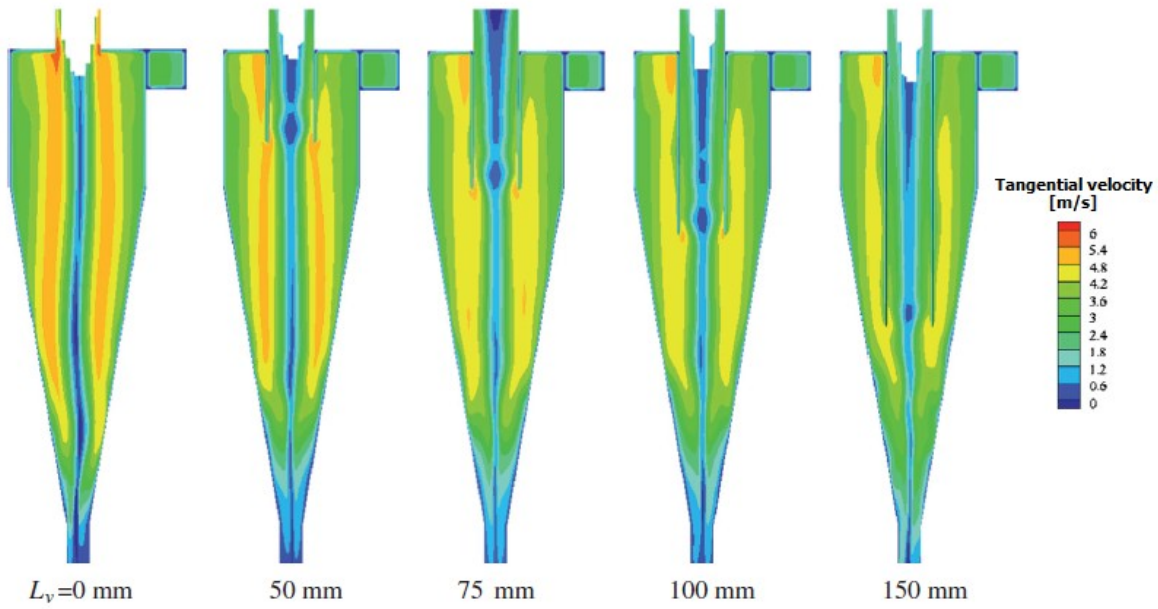

Figure 10: Tangential velocity distribution for different VF lengths (L_v) at a feed solids concentration of 30 vol% [11]

The next discussed design variable is the cylinder section. By increasing the length of the cylinder section the tangential velocity is reduced over the length and the retention time gets longer.[1] However, the difference is very small on separation performance.[12] For base conditions the cylindrical section length is as large as the hydrocyclone diameter.[10]

The cone angle impacts the residence time and the tangential velocity (see Figure 11). Decreasing the cone angle will increase the length of the cone section by fixed diameter and vice versa. A longer cone section results in longer retention time, and hence, in a finer and sharper separation.[10] Due to the small separating space with a short cone, particles probably would rebound on the contracting wall to the inner upward flow because of the increased included angle. The decrease in the length of cone has an effect of increasing the air core diameter and consequently decreasing the volume of underflow or split ratio.[12]

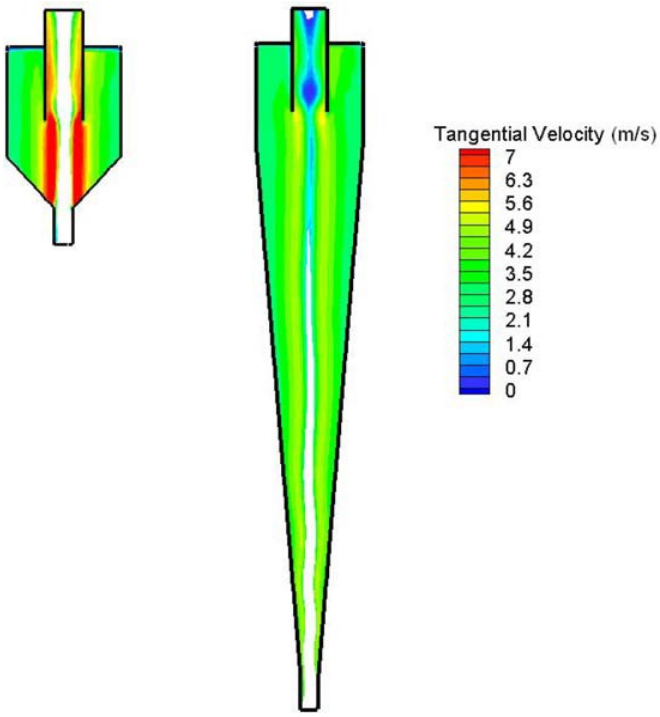

Figure 11: Tangential velocity distribution for a short and a long cone section [12]

Hydrocyclones with different cone sections are shown in Figure 12. Traditionally, cone sections have a single cone angle. Krebs developed special cone sections which offer combination of cones with different angles to gain significantly finer separation. This design is called gMAX. It consists of a steep upper cone for accelerating the slurry. Next, a long conical section with increasing cone angles is followed. It provides a long residence time in a high velocity area.[7] For base conditions the cone angles are about 12° if the hydrocyclone diameter is smaller than 10 inch. For larger hydrocyclones it is around 18-20°.[10]

In the mineral industry 20° cones are widely used for classification. Two special types with cone angles of 90° and 180° have been discussed in chapter 2.3.

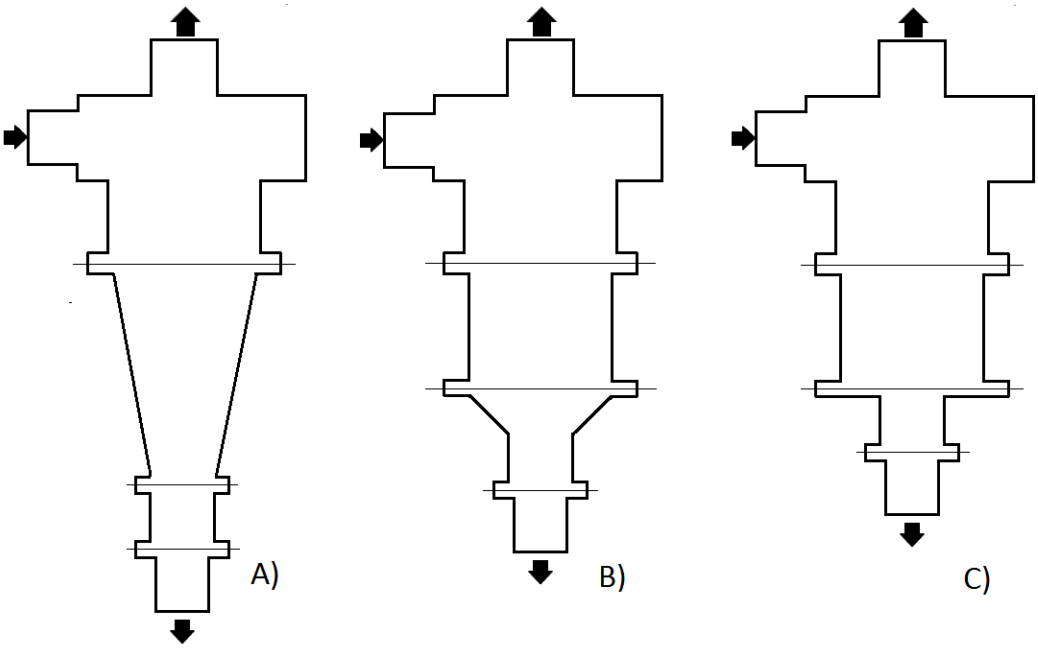

Figure 12: Hydrocyclones with different cone angles; A) 20° cone, B) 90° cone, C) flat bottom cone

The apex can differ in size in terms of the diameter as well as in the direction it is installed. Changing the apex size barley affects the separation performance because the change influences only the solids content of the underflow stream and not the separation area (see Figure 13). The size of the apex is selected to provide an underflow discharge with high solids content. The underflow solids content should be as high as possible without plugging the apex. The higher it is the less water and therefore entrained fines are in the underflow. It is important to have a discharge in form of a cone of about 20-30°, which indicates an optimum function. If it is showing a roping discharge it shows that the apex is too small. Solids cannot discharge properly and there is a risk of misplaced coarse material in the overflow. A spray discharge indicates that the apex is too large. Therefore it is too much water and consequently fines in the underflow.[7] The effect on the separation by installing the apex upside down is pursued in this thesis (see chapter 4.3.3). Conventionally an apex diameter is around 0.1-0.35 times the hydrocyclone diameter.[10]

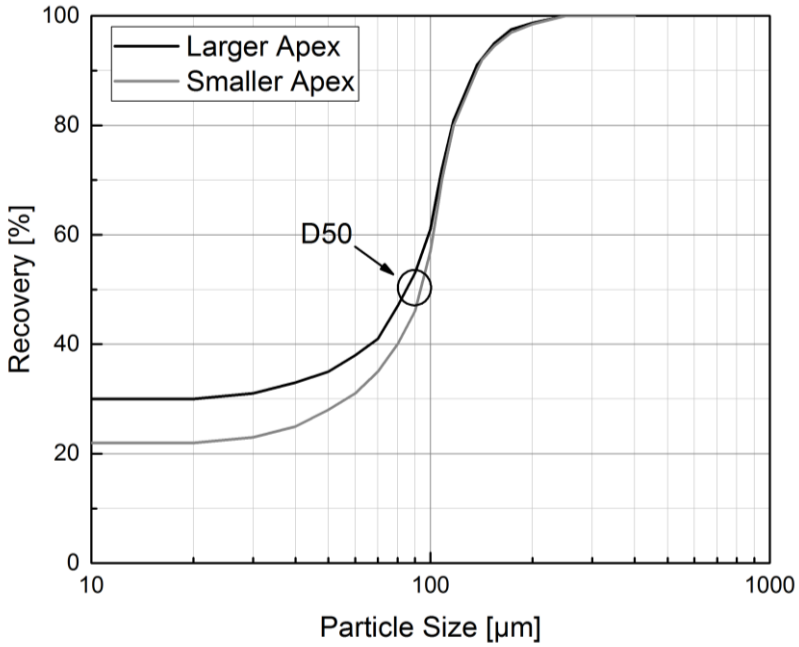

Figure 13: Effect of changing the apex size

The last discussed design variable is the mounting angle of the cyclone. The most common use of angular mounted cyclones is found at large grinding circuits, where they are installed at 45° from horizontal. A higher underflow solids content compared to vertically mounted hydrocyclones can be achieved because apex diameter is not as critical as in vertical installations. Additionally, the lower head results in reduced velocity of the slurry and therefore coarser separation.[1] For the same separation as for vertically mounted cyclones additional feed dilution water is needed. The lower head allows also reduced pump head requirements. Another advantage is the low wear in the lower cone section and apex section due to a lazy swirl discharge instead of a forced spray discharge.[9]

2.4.2. PROCESS VARIABLES

Process variables which influence the performance will be discussed next. The variables described include the density of liquid and solid, the slurry viscosity, the solids concentration and the pressure drop.

The terminal settling velocity is affected by the densities of liquid and solid. The higher the difference the finer is the separation. It has to be considered that particles with equal terminal settling velocity cannot be separated by a hydrocyclone.[7]

The slurry viscosity has a big influence on the D50, although it is the most unknown variable due to difficult measurement with coarse solids. It depends on the viscosity of the process

liquid, the slurry density and the particle size distribution. The viscosity increases with the fineness of the particles and with increasing slurry density. Viscosity and the slurry density as well as the solids concentration are not independent and therefore it is difficult to isolate their effects on separation.[7]

By increasing the solids content, the sharpness of separation decreases and the cut point rises. Figure 14 shows the effect of solids content on the D50. The reasons for the rising D50 are the greater resistance to the swirling motion as well as the increasing degree of hindered settling and viscosity within the hydrocyclone.[5]

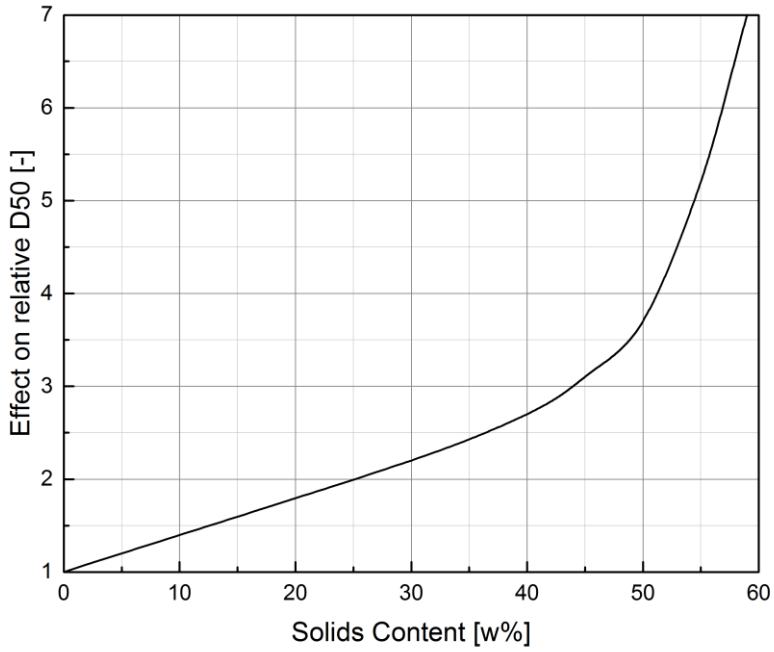

Figure 14: Ratio of solids content versus relative D50 [5]

The last discussed process variable is the pressure drop. The pressure drop across a cyclone is measured by taking the difference between the feed pressure and the overflow pressure. Normally, the overflow as well as the underflow is discharged at atmospheric pressure. So for most applications the feed pressure is the pressure drop. It is proportional to the inlet velocity at a given inlet head diameter. An increase in pressure drop leads to an increase of the centrifugal force effect which results in a finer relative D50 as seen in Figure 15. The change has to be large for a significant effect.[5]

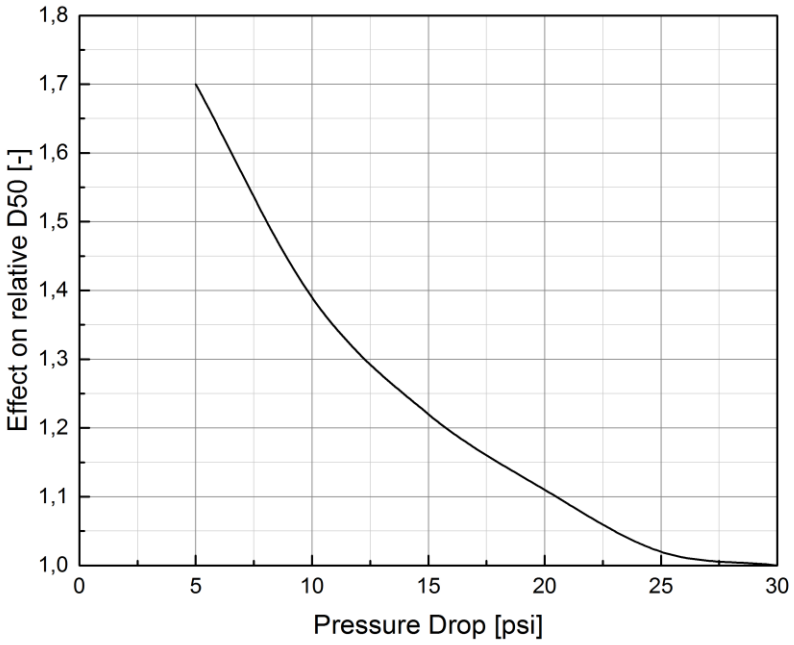

Figure 15: Ratio of pressure drop to relative D50 [5]

2.5. MODELS FOR CALCULATING HYDROCYCLONE PERFORMANCE

There exist fundamental models and empirical or semi-empirical models for hydrocyclone performance.

Fundamental models are based on describing the fluid flow and particle motion. They have difficulties in describing satisfactorily the interactions between particles and between particles and fluid while operating at high solid concentrations. Examples for fundamental models are the equilibrium theory, residence time theory and crowding theory.[3]

The equilibrium theory assumes an equilibrium orbit of particles where their terminal settling velocity radially outward is equal to the radial velocity of the liquid inward. The cut size is defined by particles that have an equilibrium orbit that corresponds to the locus zero of vertical velocity. Short residence times, high solids concentrations and different hydrocyclone geometry as used in the specific test work may result in unreasonable predictions.[3, 7]

The residence time theory assumes non equilibrium conditions and determines whether the residence time in the hydrocyclone allows a particle to reach the outer wall of the hydrocyclone. High solids concentrations and different hydrocyclone geometry as used in the specific test work may result in unreasonable predictions.[3, 7]

The crowding theory suggests that at higher feed concentrations the cut size is primarily a function of the capacity of the apex and the particle size distribution of the feed. The difficulty is that the effect of the underflow concentration cannot be described quantitatively and the conditions of the cutoff point are volatile.[3, 7]

The computational fluid dynamics (CFD) model is a numerical method. It is a preferred tool for fundamentally based modeling of hydrocyclone performance. "*Complete flow modeling of the hydrocyclone involves predicting the liquid-phase velocities, the slurry concentration profile, the turbulent viscosities and the slip velocities of particles with respect to the liquid phase for a range of particle sizes before predicting the partition curve.*" [3, p.1823-1824] The obtained fluid flow equations are nonlinear, simultaneous partial differential equations. Advances in CFD modeling such as numerical methods or computing resources are enhancing possible applications.[3]

Empirical models search relationships between experimental results and physical variables. These relationships are expressed in reasonable equations. For describing the separation, parameters of the corrected partition curve, like sharpness and cut size, are used. Empirical models are generally used for industrial hydrocyclone modeling and simulation and are the most commonly used technique.[3]

An example for an empirical model is developed by Lynch and Plitt. The model is based on regression analysis of test data. A difficulty is to predict performance when a different geometry of hydrocyclones as used for the test data is given.

Another example for an empirical model is developed by Krebs. It will be presented in the remaining paragraphs of section 2.65. It is based on test data in closed circuit copper grinding.[7]

Each size of hydrocyclone has a base D50 for standard operating conditions. These standard conditions are:[1]

- Water as feed liquid at 20 °C and a viscosity of 1 mPa·s
- Feed solids at a density of 2.65 g/cm³ and the shape of spheres
- Feed solids content of less than 1 w%
- Pressure drop of 10 psi (0.69 bar)
- Geometry of a standard hydrocyclone which means a vortex finder diameter of 30% of the hydrocyclone diameter, a feed orifice of 7% of the feed chamber area, 20° cone for larger hydrocyclones, cylinder section and vertical mount

The calculation of the predicted D50 ($D50_{actual}$) is based on following formula:[1]

$$\boldsymbol{D50_{actual} = D50_{base} * C_{VF} * C_{\text{Inlet } Head} * C_{Slurry\ Density} * C_{Pressure\ Drop} * C_{Solid\ Liquid} * C_{var}} \quad (2.8)$$

The first thing to calculate for determining the cut size for a given cyclone is the base D50 with following formula:

$$\mathbf{D50_{base} = 5.27 * D_{cyclone}^{0.66}} \quad (2.9)$$

Then, the base D50 has to be corrected for settings differing from base conditions. Therefore formulas exist for the VF, inlet head, terminal density, pressure drop and density of liquid and solids. The correction factors for the VF and the inlet head are represented as follows:

$$\boldsymbol{C_{VF} = \left(\frac{D_{VF}}{0.3 * D_{cyclone}^2}\right)^{0.6}} \quad (2.10)$$

$$\boldsymbol{C_{Inlet\ Head} = \left(\frac{A}{0.05 * D_{cyclone}}\right)^{0.15}} \quad (2.11)$$

The area of the inlet orifice is represented with A.

The correction factor for the solids concentration in the feed is probably the most important one because of the big influence on separation performance. Figure 16 shows three different curves depending on different size and viscosity characteristics. Since it is a relative measure of slurry viscosity it is affected by for example size and shape of particles. It is called terminal density correction factor because the terminal density is a value used by Krebs for viscosity correction. The terminal density value decreases with increasing viscosity.

The formula for the standard curve (Figure 16) is applicable for most applications with a broad particle size range and is represented as follows:

$$\boldsymbol{C_{Terminal\ Density} = \left(\frac{53 - V\%}{53}\right)^{-1.43}} \quad (2.12)$$

The feed solids concentration is represented by V%. The tailings curve on the left side of Figure 16 is used for very fine material and a high concentration of clays. The most right curve is used for coarse closed circuit grinding producing a coarse product. However, it should be remarked that the influence of the terminal density correction factor seems to be too important to reduce it to only three curves. If possible the terminal density correction factor is calculated backwards from known settings.

The correction factor for the pressure drop is based on following formula:

$$C_{Pressure\ Drop} = 1.91 * \Delta p^{-0.281} \quad (2.13)$$

The formula of the correction factor for density of solids and liquid is based on the Stokes Law:

$$C_{Solid\ Liquid} = \left(\frac{1.65}{\rho_s - \rho_l}\right)^{0.5} \quad (2.14)$$

Beside the mentioned variables, also numerous other variables have an influence on the D50. Some examples are cone angle, cylindrical section, mounting angle and circulating load. However, those variables may be neglected for estimating purpose.[1]

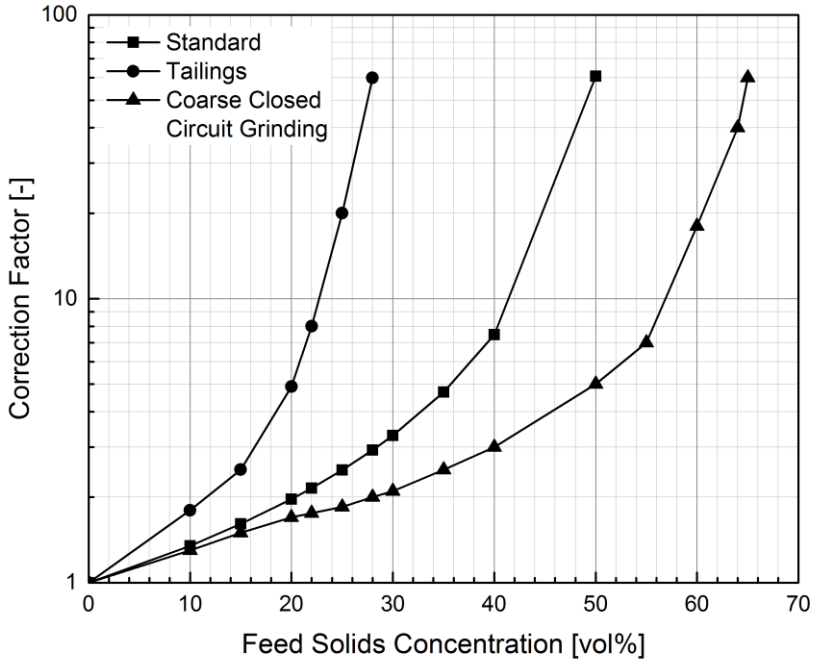

Figure 16: Correction factor for feed solids concentration depending on the type of material [1]

2.6. PARTITION CURVE

The commonest way to describe performance of a hydrocyclone is the partition curve. It relates the weight fraction of each particle size of the feed which reports to the underflow or overflow respectively to the particle size. Mostly used is the underflow related partition curve. The partition numbers are calculated as follows:

$$T_{\mu j} = \frac{r_{mj} \bullet m_{\mu j}}{m_{\mu 0}} \quad (2.15)$$

By drawing the partition numbers in a graph for particle size classes a step function results. For infinite small intervals of particle size analysis, the partition or recovery curve evolves. For forming a curve out of the step function different approaches have been established. One approach is the recovery curve approximated by the Lynch-Rao equation:

$$T_{\alpha(d)} = \frac{e^{\alpha * d/D50} - 1}{e^{\alpha * d/D50} + e^{\alpha} - 2} \quad (2.16)$$

The alpha value (α) can be selected to change the shape of the recovery curve. The curve is symmetrical around the D50 point as well as the upper and lower tails of the recovery curve.[7]

The so called D50 or cut size is the size where 50 percent of the particles present in the feed report to the underflow. So particles with this particle size have the equal chance reporting to the underflow or overflow. The sharpness of the separation can be seen at the slope of the central section of the partition curve. The steeper the slope, the sharper is the separation. For the calculation of the sharpness different approaches have been established. One definition is the Ecart Probable E_P, which is defined as follows:

$$\boldsymbol{E_P = \frac{d_{75} - d_{25}}{2}} \quad (2.17)$$

The d_{75} or d_{25} are the particle sizes with partition numbers 75 and 25 percent, respectively. The ideal separation would have a value of 0 for the E_P. Due to the reason that it is a value with a dimension, dimensionless formulas for better opportunities to compare have been approached as well. Namely, the definitions named Imperfection I and Variation $\mathcal{X}$, as in the following formulas:

$$\boldsymbol{I = \frac{d_{75} - d_{25}}{2 * d_{50}}} \quad (2.18)$$

$$\boldsymbol{\mathcal{X} = \frac{d_{75}}{d_{25}}} \quad (2.19)$$

The ideal separation would have a value of 0 for the Imperfection and a value of 1 for the Variation. It has to be remarked that E_P, I and $\mathcal{X}$ ignore the separation above partition number 75 percent and below 25 percent.[2] Another approach used in this thesis is the alpha value seen in formula 2.16. The larger the α value, the sharper is the separation. The α value for conventional hydrocyclone operations ranges from 3.5 to 4.5.[7]

2.6.1. CORRECTED PARTITION CURVE

In consequence of entrainment, a certain amount of solids reaches the underflow not through classification but rather due to short-circuiting. This behavior is observed at the partition curve not being virtually zero at the ordinate. To properly describe the quality of the separation despite entrainment it is required to adjust the partition curve to a so-called corrected partition curve. Figure 17 compares the actual with the corresponding corrected partition curve. For the corrected partition curve it is suggested that particles of all sizes are entrained in the underflow liquid by short-circuiting in direct proportion to the fraction of feed liquid reporting to the underflow. The corrected mass fraction of a particular size reporting to underflow is calculated by:[5]

$$y_{UF,i,corr} = \frac{y_{UF,i} - R}{1 - R} \tag{2.20}$$

R denotes the fraction of the feed liquid which is recovered in the underflow.

It should be noted that particles of all sizes are entrained by short circuiting nevertheless the amount of fines is much larger than the amount of coarse particles.[5]

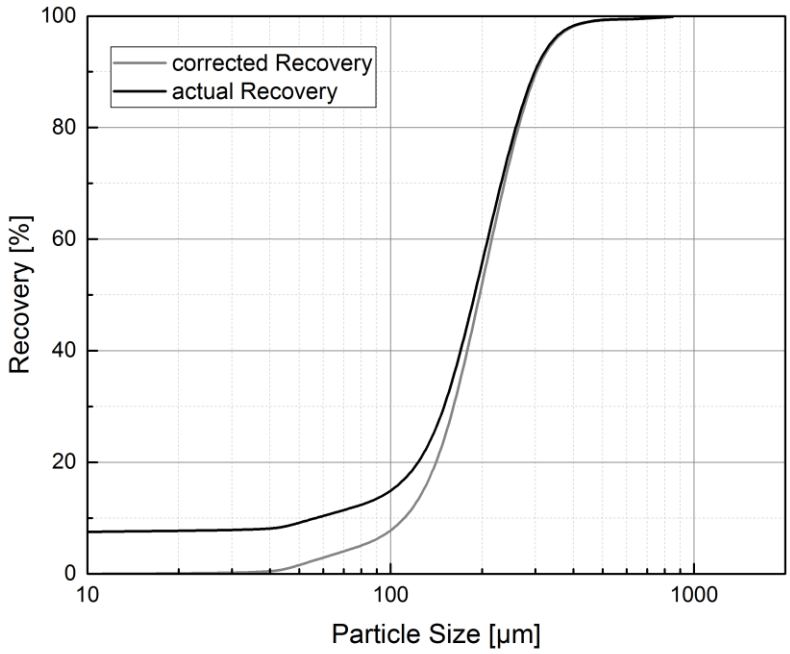

Figure 17: Comparison of corrected and actual partition curve

2.6.2. REDUCED PARTITION CURVE

For comparison of separation performance independent of hydrocyclone diameters, outlet dimensions or operating conditions the so-called reduced partition curve is developed. It is obtained by plotting the corrected weight fraction of particles reporting to the underflow versus the actual particle size divided by the corrected D50.[5] Investigations have shown that for similar cyclone designs it is constant over a wide range of diameters and depends on the material characteristics.[13]

3. EXPERIMENTAL DESCRIPTION

The experiments were made in the hydrocyclone laboratory of FLSmidth Krebs in Tucson, Arizona, USA. The number of tests amounts to 70. Two people were needed for each test series to take simultaneously and isochronously samples at the underflow and overflow.

3.1. TEST MATRIX

The test matrix was chosen to compare the separation performance of special types of hydrocyclones, namely the water-only cyclone (WOC) and flat bottom cyclone. The same settings were changed for both types. In addition, tests with a standard hydrocyclone were made to act as reference. The test matrix is shown in Table 1. The upside down installation of the apex is denoted with USD in the apex diameter column.

Table 1: Test matrix

Test Number	Pressure Drop [psi]	Vortex Finder Diameter [inch]	Vortex Finder Length [inch]	Apex Diameter [inch]	Shortcut
1-5	5;10;15;20;25	4	10	1.5	Standard Cyclone
6-10	5;10;15;20;25	3	10	1.5	
11-15	5;10;15;20;25	4	10	1.5 USD	Water-only cyclone
16-20	5;10;15;20;25	3	10	1.5 USD	
21-25	5;10;15;20;25	4	14	1.5 USD	
26-30	5;10;15;20;25	3	14	1.5 USD	
61-65	5;10;15;20;25	4	14	1.5	
66-70	5;10;15;20;25	4	10	1.5	
31-35	5;10;15;20;25	3	10	1.5	Flat bottom cyclone
36-40	5;10;15;20;25	3	14	1.5	
41-45	5;10;15;20;25	4	14	1.5	
46-50	5;10;15;20;25	4	10	1.5	
51-55	5;10;15;20;25	4	10	2.5	

The feed solids content was chosen for all tests to be about 51 w%. For the last five tests (number 66-70) the feed solids content was about 48 w% due to material shortage. The reason for the choice of the high content is following applications in a grinding circuit.

The range of the pressure drop values is also following conventional industry applications for hydrocyclone classification.

The apex and the vortex finder are relative simple replaceable parts on an installed hydrocyclone and the influence on the separation can be significant. There is no necessity

to demount the whole device for changing those parts. Different vortex finder diameters and lengths as well as different apex diameters and apex installations were tested. The tests with a vortex finder diameter at 4 inch and 3 inch were performed with all three types of cyclones. The vortex finder lengths amount for the long vortex finder length to 14 inch and for the standard vortex finder length to 10 inch. The long VF length was tested with the flat bottom and the WOC. The different vortex finder sizes used are shown in Figure 18. The vortex finder diameter to apex diameter ratio is 2.67 and 2.00. One test series of the flat bottom cyclone (test 51-55) was made with an apex diameter of 2.5 inch.

Figure 18: Vortex finders f.l.t.r.: 3 inch short, 4 inch short, 3 inch long, 4 inch long

The installation of an upside down apex is based on the application in the coal industry, where it is tried to have less gangue material in the overflow by building up a bed with the solids similar to the principle of the flat bottom and water-only cyclones discussed in 2.3. In the hard rock industry it is used as well to reach a higher solids content in the overflow (according to Krebs).

3.2. EQUIPMENT

The whole equipment is owned, designed and produced by Krebs. This includes the test rig, the hydrocyclones and the sample cutters.

3.2.1. HYDROCYCLONES

Table 2: Key features of hydrocyclones

	Standard cyclone	Water-only cyclone	Flat Bottom cyclone
Diameter [mm]	261.94	241.30	261.94
Inlet design	Ramped involute	Standard involute	Ramped involute
Inlet orifice [cm²]	54.19	50.32	54.19
Cone angle [°]	20	90	180
Cone length [mm]	423	100	241

The standard cyclone consists of a ramped involute designed (see Figure 20) entry section with a diameter of 261.94 mm (10.31 inch). The cone section has 20° angle in the length of 423 mm (16.65 inch) and is composed of two parts.

The water-only cyclone consists of one cylinder section and the standard involute designed (see Figure 20) entry section. The size of the diameter is 241.30 mm (9.5 inch). The cone section has a length of 38 mm (1.5 inch) and an angle of 90°.

The flat bottom cyclone has a ramped involute entry with a diameter of 261.94 mm (10.31 inch). The cylinder section has a length of 482 mm (18.98 inch). The cone section is simultaneously the cylinder section since the angle amounts 180°.

The three hydrocyclones are shown in Figure 19. The exact measurements are available in the technical drawings in the appendix (page 58, 59, 60).

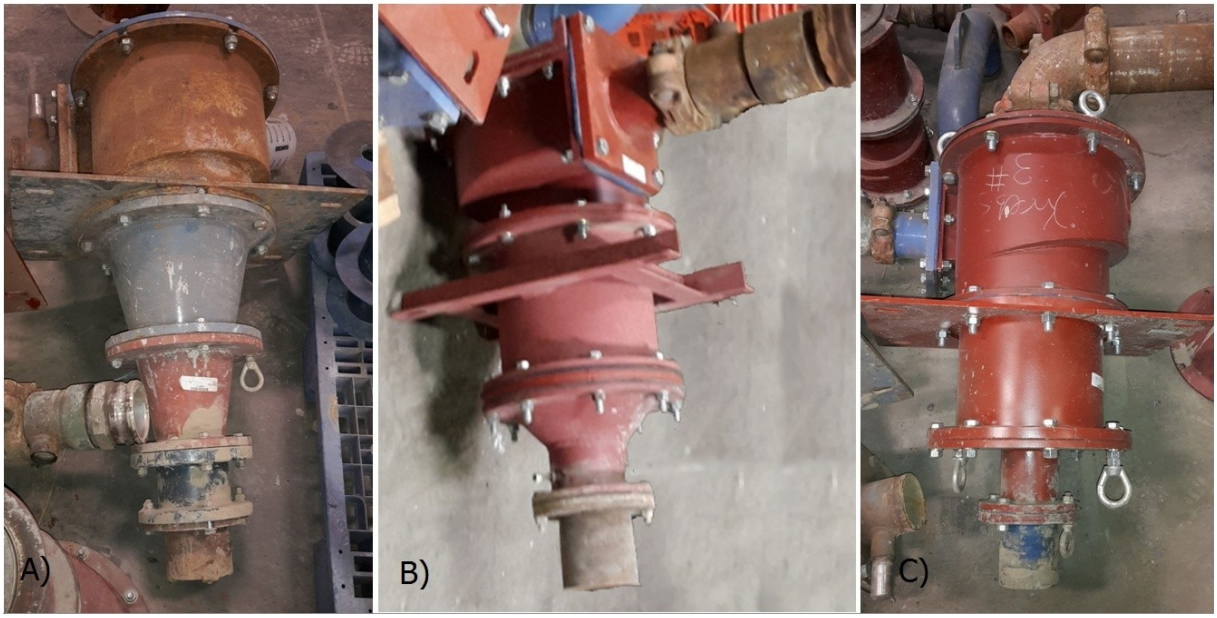

Figure 19: A) Standard hydrocyclone, B) Water-only cyclone, C) Flat bottom hydrocyclone

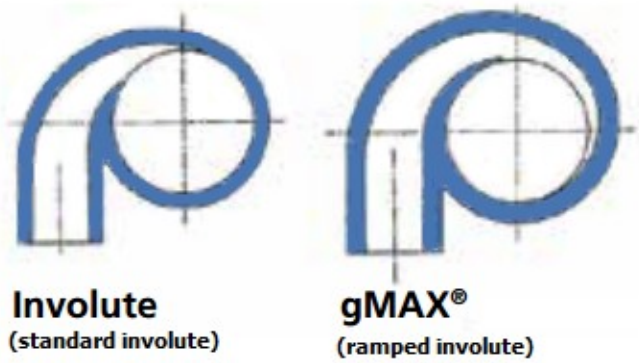

Figure 20: The profile of the used inlet designs by Krebs [14]

3.2.2. TEST RIG

The test rig operated in closed circuit. In Figure 21 and Figure 22 the test rig is seen with standard hydrocyclone installed. The pump was a Krebs millMax pump driven by a 26.68 kW motor. The feed pressure was set by controlling the speed and torque of the motor. An agitator was mounted in the pump sump to ensure suspension of the solids. The pump sump was filled up to 568 l. A pressure gauge was mounted on the feed tube right before the hydrocyclone. The overflow and underflow streams were discharged freely into the pump sump.

Figure 21: Test rig from the view of the pump

Figure 22: Test rig from the front view

3.3. FEED MATERIAL

The feed material was a mixture of tailings. The tailings from three different mines were mixed to get a broad size distribution. The mines are a silver and copper mine from Montana, a copper and molybdenum mine from Arizona and a silver mine from Mexico. The size distribution of the feed material is shown in Figure 23 and Table 3. The density of the solids was measured by fluid pycnometer and amounts to 2.80 g/cm³.

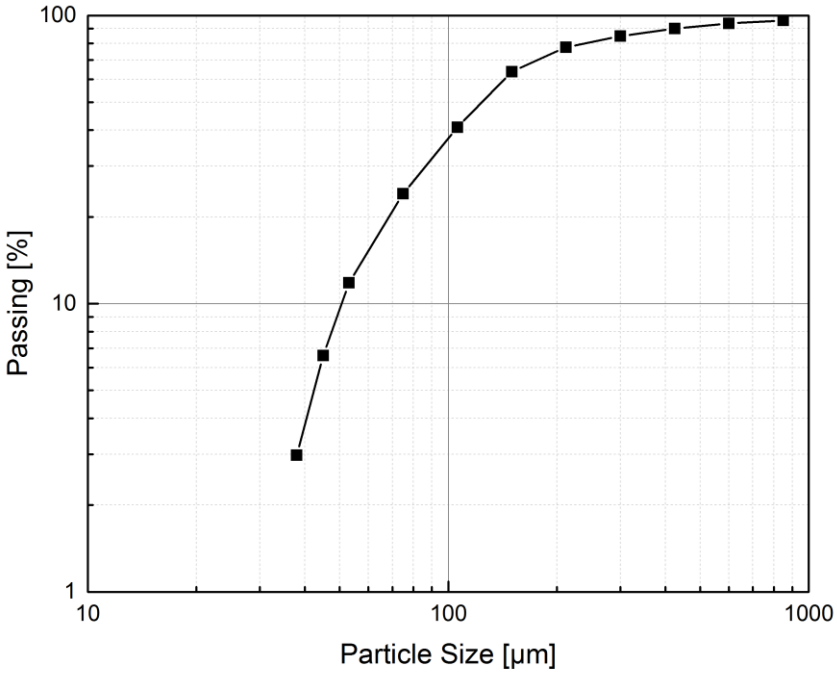

Figure 23: Particle size distribution of feed material by sieve analysis

Table 3: Particle size distribution of feed material

Particle Size [µm]	Passing [%]
850	96.00
600	93.81
425	90.00
300	84.82
212	77.50
150	63.74
106	40.89
75	24.07
53	11.81
45	6.60
38	2.98

3.4. SAMPLING

The samples were taken at the red crosses in the sketch (see Figure 24). The samples were taken with a sample cutter, which is specifically developed by Krebs (see Figure 25). The exact measurements for the sample cutter can be checked at the appendix page 61. The sample cutter was swung under the slurry stream and cut the whole stream with one continuous sweep. Because of the narrow gap the sample cutter is not filled immediately and therefore some swings are necessary which leads to a representative sample. The feed solids content was checked by taking a sample with the sample cutter at the underflow at such low pressure that no overflow stream arose. The obtained sample was filled in a cylinder glass with known volume and weighed. The resulting pulp density was used to calculate the feed solids content $c_{s,feed}$ by:

$$\boldsymbol{c_{s,feed}} = \frac{\boldsymbol{\rho_s}*(\boldsymbol{\rho_l}-\boldsymbol{\rho_p})}{\boldsymbol{\rho_p}*(\boldsymbol{\rho_l}-\boldsymbol{\rho_s})} \tag{3.1}$$

If it was not reaching about 51 w%, either more material or water was added to the system and determined again. After checking the feed solids content the pressure drop was increased to 5 psi. At the beginning of the sampling of every test series (i.e. at 5 psi), the apex discharge was checked for anomalies and recorded by photography. If no anomalies were noticed, a splash skirt was added and the sampling began. The samples of overflow and underflow were taken with the sample cutters. The samples were taken simultaneously and for the same amount of time. Hence, the masses of the samples of overflow and underflow were weighed. Subsequently, the mass flow rates were measured. Therefore a stopwatch, a yardstick and buckets with known cross sectional area were used. The flow rate of the underflow was measured by holding a bucket under the stream as long as it was nearly full but not overflowing while measuring the time. For measuring the volume the yardstick was held in the bucket and the length was multiplied by the cross sectional area. For measuring the flow rate of the overflow, the moveable hose was pushed to the discharge tank which led to a bucket while measuring the time. When the bucket was nearly full the hose was pushed back to the pump sump and the time measurement was stopped. The volume was measured the same way as for the overflow bucket. The samples of the overflow and underflow were wet pre-screened at 38 µm to reduce fines for dry screening. Then they were dried in the oven by 176.7 °C (350 °F) for 24 hours. The screening of the dry material took place in a sieve shaker. The sieve stack contained 11 sieves with mesh sizes of: 850 µm, 600 µm, 425 µm, 300 µm, 212 µm, 150 µm, 106 µm, 75 µm, 53 µm, 45

µm and 38 µm. The sieve shaker was programmed to sieve for 30 minutes at a frequency of 60 hertz.

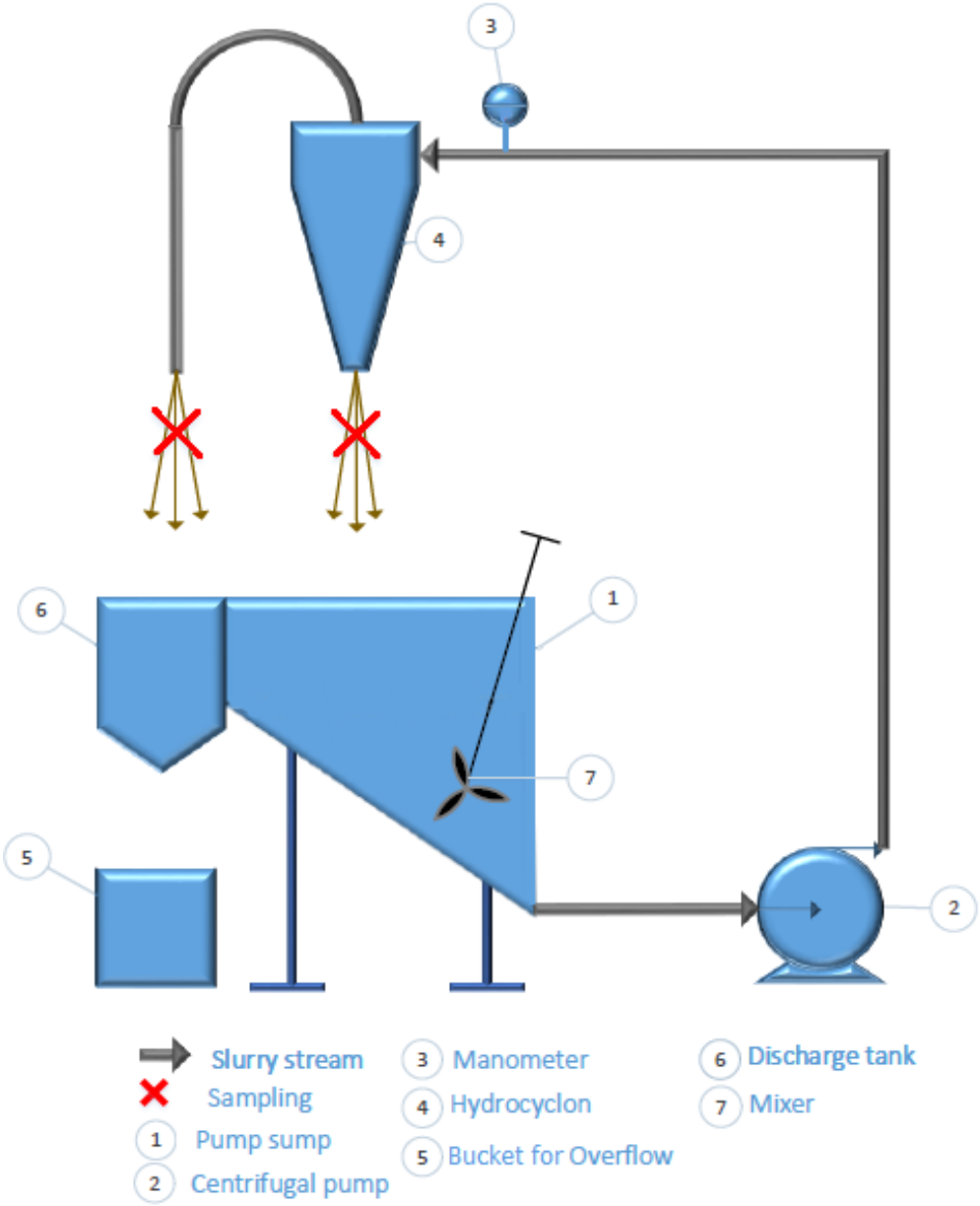

Figure 24: Schematic sketch of hydrocyclone stand

Figure 25: Sample cutters

3.5. ANALYSES

The mass balance was calculated on base of the measured mass flows, particle size distributions and solids contents of overflow and underflow. In Figure 26 an extract of the calculation sheet is shown. The known values are highlighted. The remaining values are calculated. The solids content is referred to as % SOLIDS WT. The flow rate is referred to as U.S. GPM PULP. The WATER SPLIT denotes the fraction of the feed liquid which is recovered in the underflow. The density is referred to as S.G. PULP.

SPEC. GRAVITY:	SOLIDS	2,80	LIQUID	1,00		
		FEED	OVERFLOW		UNDERFLOW	WATER-SPLIT
STPH SOLIDS		58,4	41,2		17,2	7,7
STPH LIQUID		53,5	49,4		4,1	
STPH PULP		111,9	90,6		21,4	
% SOLIDS WT		52,2	45,5		80,7	
S.G. PULP		1,5	1,4		2,08	
% SOLIDS VOL		28,1	23,0		59,9	
U.S. GPM PULP		297,5	256,4		41,1	
cyclone.wk4 Ver 4.1				% CIRCULATING LOAD	41,8	

Figure 26: Extract of calculation sheet

A whole calculation sheet used is shown in the appendix (page 50). The actual recovery was calculated with the flow rates of the underflow and the feed for each particle size. The corrected recovery was calculated by:

$$E_{UF,corr} = \frac{E_{UF} - \text{Water Split}}{100 - \text{Water Split}} \quad (3.2)$$

For drawing the corrected recovery curve the mathematical model by Rao-Lynch (see formula 2.16) is used. By non-linear regression, the D50 and α value are approximated until the correlation coefficient reaches a maximum. The curve is drawn on base of the new calculated D50 and α value. An example is illustrated in Figure 27. The points of the corrected recovery curve are shown in the diagram as well.

As the calculation of the partition numbers uses the mass fractions of particle size classes, the resulting figures are an average for the entire size class. This implies that every class contains particles with both lower and higher partition numbers. Therefore the calculated partition numbers are usually plotted at either the arithmetic or geometric average of the particle size class. However, it is common practice at FLSmidth Krebs to plot it at the lower particle size limit. Adhering to this practice also in this thesis maintains the possibility for comparison of the present data with historical data in the company.

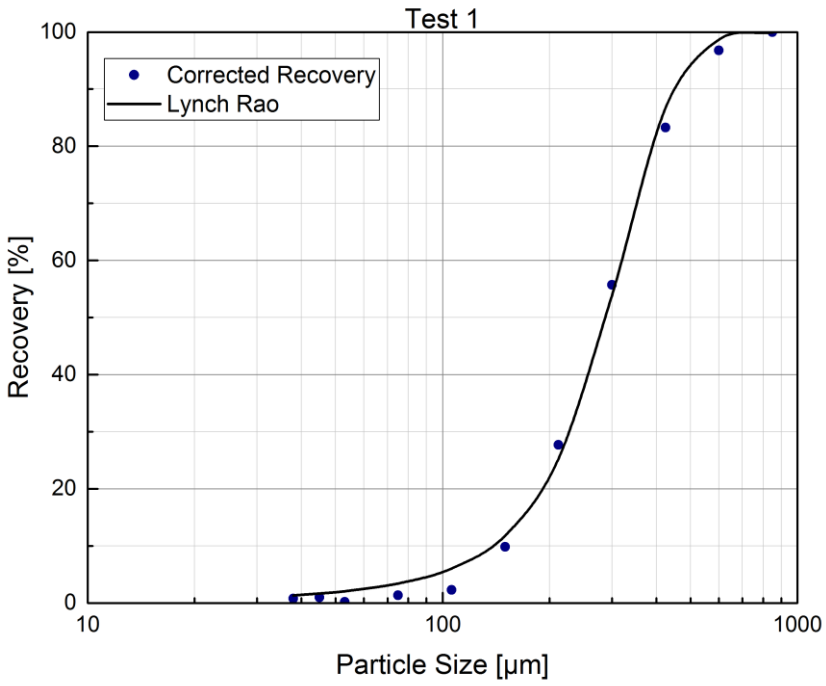

Figure 27: Example for efficiency curve

Beside the calculation of the separation performance, additionally the Krebs prognosis model was applied. Since the design parameters of the flat bottom and WOC differ widely from the standard hydrocyclone, the prognosis model was only applied for the standard hydrocyclone. The calculation was made for the first test series (test 1-5). For calculating the correction factors the formulas 2.9, 2.10, 2.11, 2.12, 2.13 and 2.14 were used. Those results were applied to formula 2.8.

4. RESULTS AND DISCUSSION

Table 4 shows the D50, alpha value and underflow solids content of each test.

Table 4: Results of all tests in terms of D50, alpha and underflow solids content

Test Number	D50 [µm]	Alpha [-]	Underflow solids content [%]
1	288.96	3.95	66.10
2	225.20	6.31	68.80
3	199.03	5.48	80.70
4	193.65	5.12	81.50
5	190.63	5.03	82.00
6	391.94	2.91	64.00
7	232.91	3.86	75.20
8	191.09	4.87	79.30
9	169.02	3.92	80.40
10	174.53	4.93	81.10
11	798.81	10.33	54.30
12	690.14	9.08	67.60
13	678.37	8.74	70.80
14	651.68	8.01	71.60
15	615.62	6.45	72.00
16	684.22	10.79	59.90
17	616.15	7.52	64.80
18	544.24	6.77	68.20
19	531.74	7.02	68.20
20	477.94	6.56	69.20
21	858.78	15.58	52.10
22	799.20	9.25	60.90
23	845.70	7.53	61.80
24	878.49	6.41	63.40
25	896.79	6.01	65.00
26	769.55	10.82	57.70
27	678.31	8.69	60.90
28	641.97	7.03	63.00
29	655.33	7.00	63.70
30	620.21	5.63	64.70
31	699.01	7.08	57.20
32	629.97	12.74	65.30
33	372.96	4.13	65.38
34	335.47	4.47	74.00
35	301.01	4.67	77.10
36	703.91	7.42	59.38
37	580.60	4.60	63.05
38	443.64	3.43	67.42
39	395.95	3.60	71.00
40	312.91	4.38	74.18
41	707.04	9.37	59.52
42	521.05	5.92	69.77
43	487.58	5.35	73.40
44	459.72	5.33	77.42
45	477.50	4.70	79.32
46	598.12	5.10	60.60
47	491.11	6.38	69.74
48	436.49	5.99	74.33
49	440.12	5.24	77.92
50	396.41	5.57	78.66
51	638.28	7.51	53.55
52	468.02	5.39	58.09
53	387.47	6.20	62.40
54	363.84	5.78	63.46
55	362.10	5.08	65.27
61	657.30	4.10	53.40
62	430.06	3.46	73.30
63	391.76	4.43	77.90
64	391.54	4.58	80.60
65	356.55	4.76	83.10
66	327.25	3.45	58.80
67	289,.92	4.51	74.50
68	265.71	5.01	75.50
69	271.93	4.59	79.00
70	269.58	4.93	78.80

4.1. STANDARD HYDROCYCLONE

Figure 28 shows the D50 as well as the alpha values of the standard hydrocyclone tests with a vortex finder (VF) of 4 inch diameter and 3 inch diameter along the pressure drops.

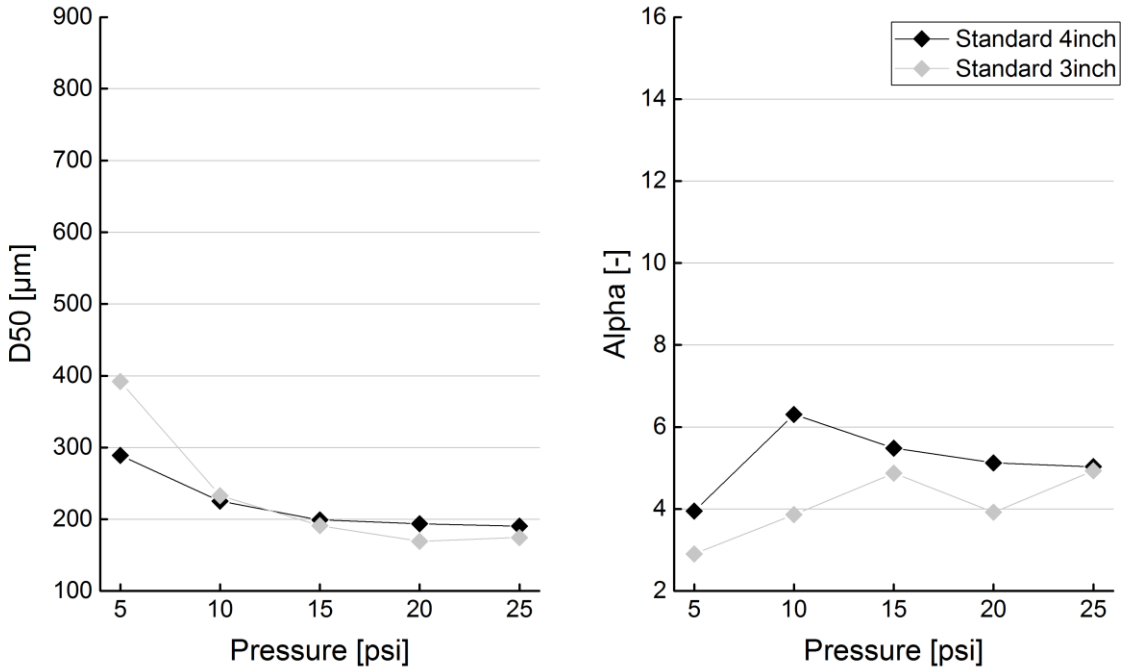

Figure 28: Results of standard hydrocyclone with VF diameters of 4 inch and 3 inch

4.1.1. VF DIAMETER

For high pressure drops the installation with the 3 inch diameter VF shows a finer separation than for the 4 inch diameter VF. The D50 for low pressure drops does not agree with the theoretical understanding that the D50 for smaller VF diameters should be also smaller. A reason for that anomaly is probably a too small pressure drop to establish an appropriate separation. Considering a very high feed solid concentration it possibly needs more pressure to overcome the greater resistance to the swirling motion.

Additionally, it can be seen that the sharpness for the smaller VF diameter installation is decreasing from 10 psi until 25 psi whereby it is rising for the larger VF diameter installation from 5 psi to 15 psi. By increasing pressure the D50 gets finer.

The underflow solids content is, as in every single test series, increasing with increasing pressure drop in the range of 66.10% to 82.00% for the 4 inch VF diameter and in the range of 64.00% to 81.10% for 3 inch VF diameter.

4.2. FLAT BOTTOM HYDROCYCLONE

Figure 29 shows the D50 and the alpha values of the flat bottom hydrocyclone tests with a VF of 4 inch and 3 inch diameter with both long and standard VF length as well as the configuration of the 4 inch diameter with the 2.5 inch apex along the pressure drops.

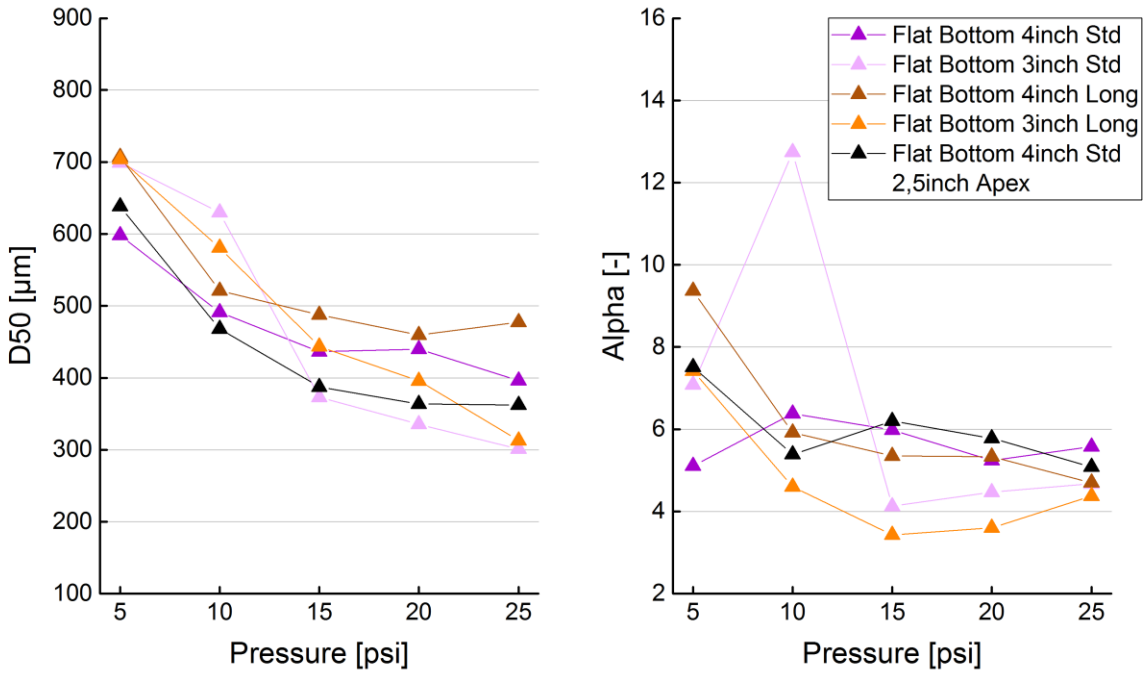

Figure 29: Results of flat bottom with a 4 inch and 3 inch VF diameter with both long and standard VF length as well as the configuration of the 4 inch diameter with the 2.5 inch apex

4.2.1. VF DIAMETER

An interesting observation is that the D50 for low pressure drops is coarser for the 3 inch VF diameter compared to the 4 inch VF diameter installation while they are finer for high pressure drops. This observation applies for both VF lengths configurations. This change is happening between 10 psi and 15 psi. Particularly striking is the big jump between 10 psi and 15 psi for the standard VF length and 3 inch diameter installation. This striking feature can be also observed at the alpha values. At the installation with the 4 inch VF diameter the biggest difference of the D50 (from 630 µm to 373 µm) appears between 5 psi and 10 psi. Both 3 inch VF montages with either the long or the standard VF length show a big change

in the D50 over the pressure starting at about 700µm at 5psi and ending at about 300 µm at 25 psi.

The assumption that the smaller VF diameter has the finer separation seems applicable for the long VF installation. Considering it is starting at the nearly same D50 the only outlier is at 10psi. The disparity of the D50 of small to large VF diameter increases by increasing pressure drop. The assumption that the smaller VF diameter has the finer separation is not applicable for the installation with the standard length where the D50 as well as the alpha values differ greatly for small and large VF diameter. Especially the alpha value at 10 psi with a value of 12.74 for the 3 inch VF diameter is quite out of range. It is considered that the value at 10 psi is an outlier and therefore not representative.

The remaining alpha values are in the range of 3.43 and 9.37. It is noticed that the alpha value at 5 psi for all flat bottom tests differs greatly from the remaining tests. An explanation could be a too low pressure drop at high feed solids content for proper separation.

The underflow solids content is increasing with increasing pressure drops and is in the range of 57.20% to 77.10% for the 3 inch VF diameter and in the range of 60.60% to 78.66% for the 4 inch VF diameter.

4.2.2. VF LENGTH

The influence of the VF length on the D50 is smaller than the influence of the diameter. The standard VF length shows a finer D50 towards the long VF length for the 4 inch diameter. For the 3 inch diameter this trend has one exception at 10 psi. The ratio of the D50 for standard to long length ranges for the 4 inch diameter between 0.83 and 0.96 and for the 3 inch diameter between 0.84 and 0.99. At the sharpness the alpha value at 5 psi for the 4 inch installation is noticeable, which is nearly twice as high for the long VF length for the 4 inch VF configuration. Apart from that the alpha values appear smaller for the long VF length except at 20 psi where it is nearly the same as for the standard VF length. For the 3 inch VF diameter configuration the sharpness is also lower for the long VF except the value at 5 psi. The reason for the lower sharpness is explained by the design. Considering the short hydrocyclone design and the long VF length, spinning coarse particles arising from turbulences at the refuse bed could be easily sucked up. This is improved by the increasing size and power of the air core with increasing pressure drop.

The underflow solids content for the long VF configurations increases for the 3 inch diameter from 59.38% to 74.18% and for the 4 inch diameter from 59.52% to 79.32%.

4.2.3. APEX SIZE

Two test series were made with the apex diameter of 2.5 inch. The tests combined with the 3 inch VF diameter where not feasible due to instable pressure drop and no appearance of the overflow. Not until reaching a pressure drop of 15 psi an overflow stream occurred. The chosen configuration was not suitable for proper operation. The tests combined with the 4 inch VF diameter could be analyzed, but as shown in Figure 30 the spray discharge indicated already a too big apex diameter in relation to the VF diameter. Figure 31 presents a discharge at normal operating conditions. The results for those tests show a slightly finer D50 for the bigger apex starting at 10 psi as seen in Figure 29. The alpha values of the small and large apex are close to each other except at 5 psi for reasons as mentioned in chapter 4.2.1.

The too big apex diameter is underlined by the low range of the underflow solids content of 53.55% to 65.27% in comparison with the other flat bottom tests.

Figure 31: Normal discharge at 2.5 inch apex

Figure 30: Spray discharge at 2.5 inch apex

4.3. WATER-ONLY HYDROCYCLONE

Figure 32 shows the D50 and the alpha values of the water-only cyclone (WOC) tests with a VF of 4 inch and 3 inch diameter with both long and standard VF length with the upside down (USD) apex installation and the 4 inch diameter with both long and standard VF length with the right side up (RSU) apex installation along the pressure drops.

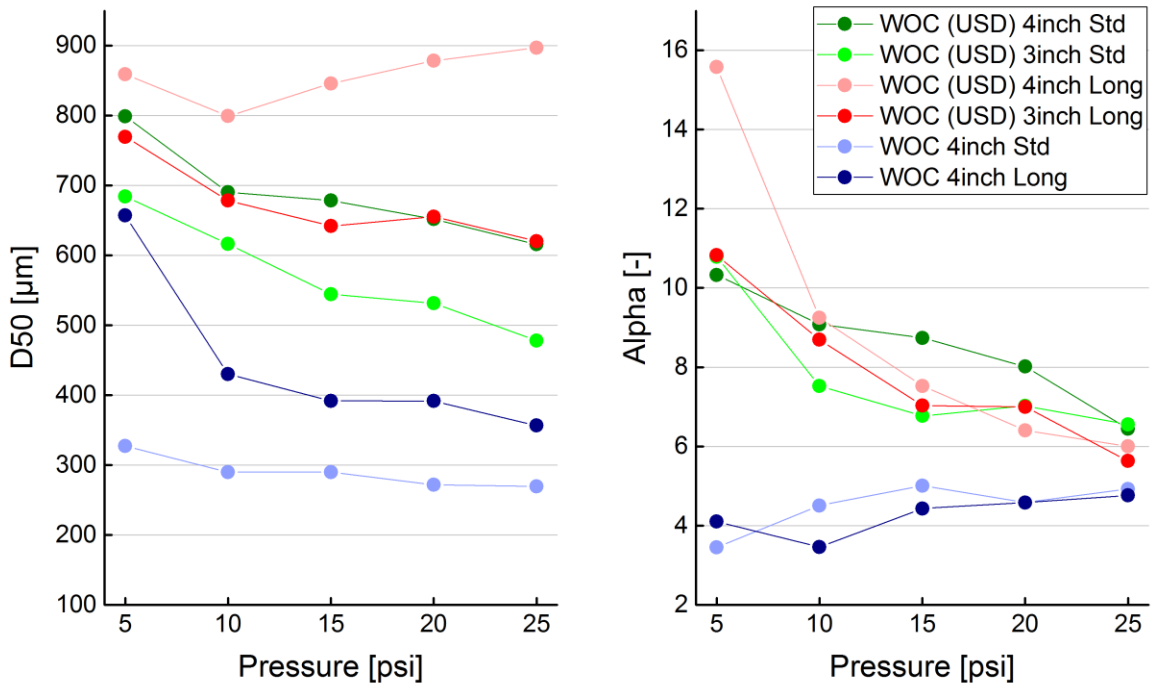

Figure 32: Results of WOC (USD) with a 4 inch and 3 inch VF diameter with both long and standard VF length configuration and WOC (RSU) with 4 inch VF diameter and both length configurations

4.3.1. VF DIAMETER

For the comparison of the VF diameters of 3 inch and 4 inch, the data from the tests with the apex installation upside down was chosen because no tests with right side up apex installation exist for both diameters.

The D50 for the bigger diameter is for both VF lengths continuously coarser than for the smaller one. The sharpness for the configuration with the standard VF length is higher at the 4 inch diameter compared to the 3 inch diameter except the test at 5 psi and 25 psi for which the alpha values are close to each other. For the configuration with the long VF length the sharpness is higher at the 4 inch diameter except for one value at 20 psi. With increasing pressure drop the D50 is decreasing as expected barring the test with the 4 inch long VF which is discussed in 4.3.2. Additionally the sharpness is decreasing as well. This is probably due to shorter retention times because of increasing velocities. Another reason could be increasing turbulence at the region of the refuse bed. Gradually arising spinning coarse particles from turbulences at the refuse bed could end in the overflow stream.

The underflow solids content for WOC (USD) for the 4 inch VF diameter is starting at 54.3% and increasing over pressure until 72%. For the 3 inch VF diameter installation it is starting

at 59.9% and ending at 69.20%. For the WOC (RSU) installation the 4 inch VF diameter has an underflow solids content of 58.80% at 5 psi rising up to 78.80% at 25 psi.

4.3.2. VF LENGTH

Comparing the 10 inch and 14 inch VF length with the right side up apex installation, the long VF has throughout a coarser D50 than the installation with the standard one. With increasing pressure the difference of the D50 between the standard and the long VF length is decreasing. The average ratio of standard to long is 0.66. Whereby, the value at 5 psi for the long VF length shows a big jump to the value at 10 psi, which indicates the same problem as mentioned before thus a too low pressure drop for proper separation. This phenomenon is not seen as clear for the installation with the standard VF length what could maybe be explained with the slightly decreased feed solids content for these five tests due to material shortage. By reason of the lower feed solids content it was probably possible to overcome the resistance of the swirling flow already at 5 psi.

The sharpness of separation is weaker with the long VF barring the test at 5 psi. Another observation is that the sharpness is slightly increasing with increasing pressure.

For the test with the apex installed upside down, the D50 for the long vortex finder is also coarser. Nevertheless, by increasing pressure drop the trend of the D50 is vice versa as with the apex installed right side up because the installation with the long VF is getting coarser by increasing pressure. This observation breaks the ranks of all remaining results. By looking at the partition curves at Figure 41 in the appendix anomalies are detected. The highest partition number of the curve of test 22 does not even reach above 64%. The partition numbers of the remaining tests ranges all below 51%. Since the partition curve for the same settings except the apex installations show a proper separation result, the poor separation performance goes back to the USD apex installation for this cyclone configuration. The high sharpness deludes since the range in which the steepness is located does not exceed a partition number of 64% and therefore is not comparable.

The underflow solids content for the WOC (USD) 3 inch long VF configuration is starting at 57.70% at 5 psi and rises up to 64.70% at 25 psi. For 4 inch long VF configuration it is 52.10% at 5 psi and increases to 65.00% at 25 psi. The WOC (RSU) 4 inch long VF installation shows an underflow solids content of 53.40% at 5 psi which is increasing until 83.10% at 25 psi. The low ranges of the underflow solids content for the WOC (USD) installation indicate a lot of water and therefore entrained fines in the underflow product.

4.3.3. APEX INSTALLATION

The apex is installed either in the right side up position or in the upside down position (see Figure 33). The two apex installations in the WOC show a significant difference at the D50 and the sharpness. The upside down installed apex for the standard VF length by an average is 2.41 times coarser than the right side up installed apex. Furthermore it shows a much sharper separation. The alpha value is 1.96 times larger for the standard VF length. This is probably attributable to the improved refuse bed caused through the USD installation. It is building a heavy media inside the cyclone and restrains small or light particles on top of the bed while coarse or heavy particles penetrate it. So the coarse separation is probably explained by particles which were carried out to the outer wall of the hydrocyclone due to centrifugal forces but then were still too small or too light for the formed heavy media and carried out through the overflow. The sharp separation could be explained by the refuse bed acting like a second separation step.

Since the effect of the refuse bed should also be present at the RSU installation it has to be underlined the assumption that the effect is not as strong as for the USD installation. Furthermore it has to be mentioned that with present data no specific explanations on the effect on separation caused by the USD apex installation can be made. Therefore, further investigations are recommended.

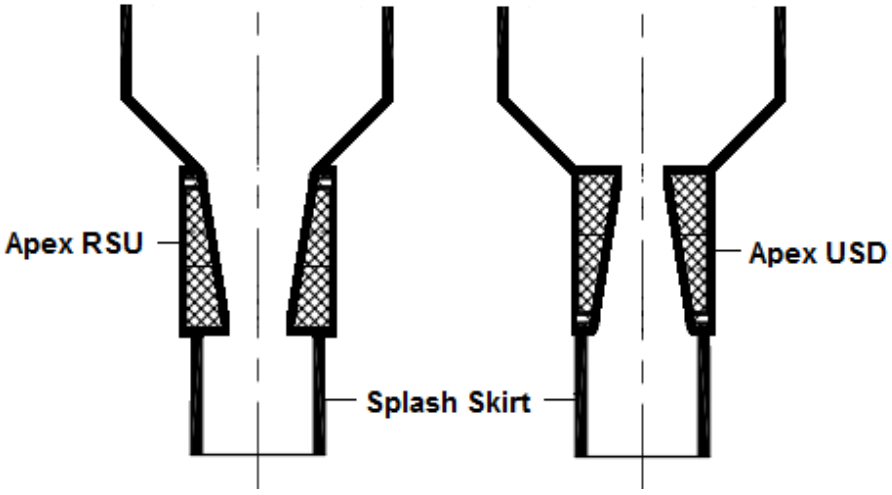

Figure 33: Apex installations

4.4. COMPARING TYPES OF HYDROCYCLONES

In Figure 34 the results for the different hydrocyclones comparing the 4 inch and 3 inch VF diameters are shown. Figure 35 shows the results for the different hydrocyclones comparing the long and standard VF lengths. The VF diameter chosen for the results in Figure 35 is the 4 inch VF since for the WOC (RSU) installation no other configurations are available.

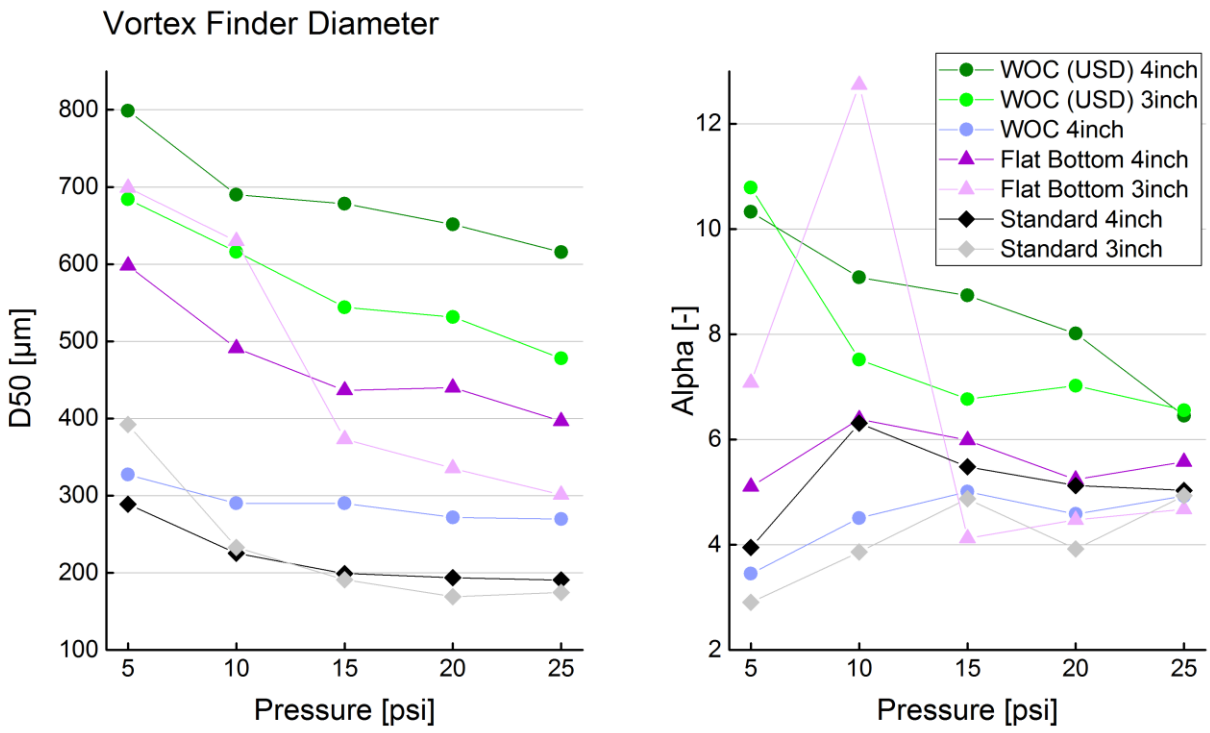

Figure 34: VF diameter results of all hydrocyclones shown with D50 and alpha values over pressure drop

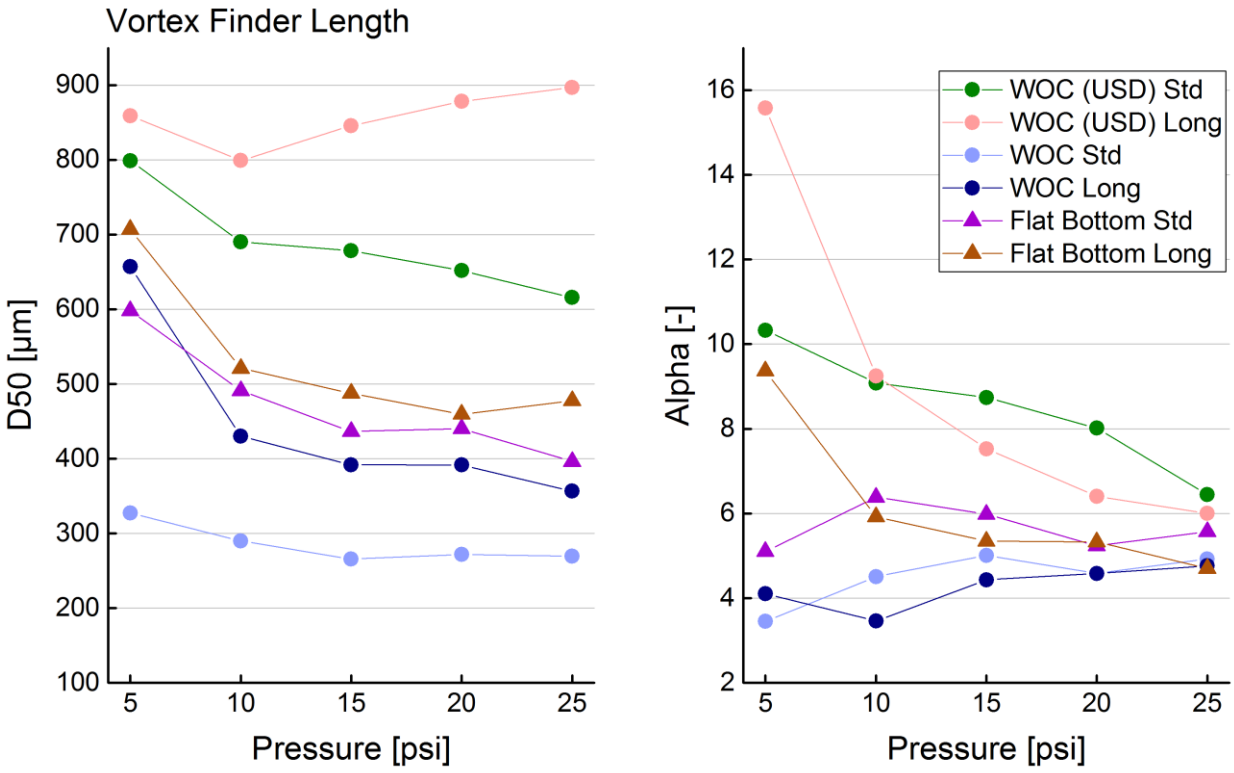

Figure 35: VF length results of all hydrocyclones shown with D50 and alpha values over pressure drop

Some general trends seen for all hydrocyclones are:

- With increasing pressure drop the underflow solids content increases
- With increasing pressure drop the separation gets finer barring one test series for the WOC (USD) with long VF discussed in 4.3.2
- The long VF installation leads to coarser separation
- The D50 and alpha values at 5 psi differ usually from those at the remaining pressure drops

The standard hydrocyclone shows the smallest disparity at the D50 by changing the VF diameters compared with the other cyclones.

The WOC with the upside down installation has by far the highest D50. The assumption that the flat bottom has the coarsest D50 did not come true. Whereby it has to be mentioned that no discussion of the performance of an USD apex installation was found in any literature and therefore the expectations were unclear. The fact that the results for the performance of

the WOC (RSU) matches the expectations, makes it clear that the USD apex installation alone causes the significant changes in separation performance.

The influence of the USD apex installation needs further investigations since with present data no specific explanations can be made.

Though, for RSU apex installations the flat bottom has the coarsest separation followed by the WOC and the standard hydrocyclone.

The average ratios of the D50 and alpha values of one hydrocyclone compared with another are shown in Table 5. The biggest difference is seen for the standard hydrocyclone compared to the WOC with the USD apex installation with the D50 ratio of 0.32 and 0.40 according to the VF diameter. The alpha value ratios between those two cyclones amount to 0.38 and 0.44. The smallest disparity for the D50 is seen for the comparison of the WOC with the RSU apex installation and the flat bottom with the 4 inch long VF with a ratio of 0.83. Although, the associated alpha value ratio with 0.74 is not the smallest difference. This occurrence is found for the comparison of the standard cyclone and flat bottom with a ratio of 0.91 for the alpha value. The D50 ratio for those both cyclones amounts to 0.46.

Table 5: Ratios for comparison of different hydrocyclone types

4 inch VF Std; 1.5 inch Apex	average D50 ratio	average α ratio
Standard/Flat Bottom	0.46	0.91
Standard/WOC (USD)	0.32	0.62
Standard/WOC(RSU)	0.75	1.16
WOC (USD)/Flat Bottom	1.47	1.52
WOC (RSU)/Flat Bottom	0.62	0.80
4 inch VF Long; 1.5 inch Apex	average D50 ratio	average α ratio
WOC (USD)/Flat Bottom	1.65	1.42
WOC (RSU)/Flat Bottom	0.83	0.74
3 inch VF Std; 1.5 inch Apex	average D50 ratio	average α ratio
Standard/Flat Bottom	0.51	0.77
Standard/WOC (USD)	0.40	0.56
WOC (USD)/Flat Bottom	1.32	1.35

4.5. PROGNOSIS MODEL

The results for the correction factors determined with formulas 2.9, 2.10, 2.11, 2.12, 2.13, 2.14 and 2.8 are shown in Table 6. The $D50_{actual}$ values represent the prognosticated D50 calculated with the formulas and the $D50_{measured}$ represents the D50 values of the performed tests.

Table 6: Results of correction factors, $D50_{actual}$ and $D50_{measured}$

	$D50_{base}$	C_{VF}	$C_{Inlet\ Head}$	$C_{Terminal\ Density}$	$C_{Pressure\ Drop}$	$C_{Slurry\ Liquid}$	$D50_{actual}$	$D50_{measured}$
Test 1	24.09	1.19	1.08	2.89	1.22	0.96	104.06	288.96
Test 2	24.09	1.19	1.08	2.59	1.00	0.96	76.60	225.20
Test 3	24.09	1.19	1.08	2.94	0.89	0.96	77.70	199.03
Test 4	24.09	1.19	1.08	3.05	0.82	0.96	74.26	193.65
Test 5	24.09	1.19	1.08	3.01	0.77	0.96	68.99	190.63

It can be seen that the measured D50 is way coarser than the predicted one for all tests. This is mostly caused by the correction factor for the terminal density. This factor has a significant impact on the $D50_{actual}$. The difficulty is the dependency on the slurry viscosity which is very hard to measure for coarse particle size distributions in liquid. In this case it is clearly shown that the standard curve does not agree with the measured results. By using the tailings curve the difference of the measured and prognosticated D50 increases even more. The calculation of the required $C_{Terminal\ Density}$ from the measured D50 reveals that the correction factor should rather be in the range between 8.36 and 9.25.

5. SUMMARY

The present thesis shows the separation performance of two different hydrocyclone types as well as the influence of design and process parameters. The cyclones used are the flat bottom and WOC, both characterized by the wide cone angle. The parameters changed are the VF diameter, VF length, apex installation, apex diameter and the pressure drop. The aim was to get a better understanding of those types of cyclones and the response of separation performance to changing parameters.

The following conclusions can be drawn from the present study:

- The USD installation of the apex shows a significant influence on the separation performance. The USD installed apex is by an average 2.41 times coarser than the right side up installed apex with same settings. Furthermore the sharpness increases 1.96 times by the USD installation. Further investigations are recommended since with present data no specific explanations on the effect on separation caused by the USD apex installation can be made.
- The poorest separation performance is shown by the WOC with the 4 inch long VF configuration and the USD apex installation. The highest partition number does not exceed 64%. Therefore also the high alpha values are not comparable.
- Longer VF length leads to coarser separation for all hydrocyclones and by looking at the trend for high pressure drops also to a less sharp separation.
- Smaller VF diameter leads to finer D50 whereby in case of the standard and flat bottom hydrocyclone this is only seen for high pressure drops. Additionally, it leads to a less sharp separation barring low pressure drops for the flat bottom cyclone. However, those values for the flat bottom at low pressure drops have to be considered with care because they differ greatly from the remaining values.
- The influence on separation by changing VF diameter is bigger as by changing the VF length.
- In general the results for the tests at 5 psi differ usually from the remaining values. This indicates the need of a higher pressure drop than 5 psi for proper separation due to the high feed solids content.
- The WOC (USD) shows both the coarsest separation as well as the sharpest.

- For RSU apex installations the expectations were fulfilled that the flat bottom has the coarsest separation followed by the WOC and standard hydrocyclone. The flat bottom has also the sharpest separation for said configuration.
- For the Krebs prognosis model the appropriate correction factor for the terminal density has to be determined since the already existing standard curve does not work for the present material characteristics.

LIST OF REFERENCES

[1] Olson T.J., Turner P.A.: Hydrocyclone selection for plant design, In: Mular A. L. et al, ed., Mineral processing plant design, practice and control, Volume 1, Vancoucer, Society for Mining, Metallurgy and Exploration Inc., p.880-893 (2002)

[2] Schubert H.: Aufbereitung fester Stoffe, Band I, 4. Edition, Leipzig, Deutscher Verlag für Grundstoffindustrie, p.239,240,277-293 (1996)

[3] Cilliers J.J.: Hydrocyclones for particle size separation, Particle Size Separation, Manchester, Academic press, p.1819-1825 (2000)

[4] Kelsall D.F.: A study of the motion of solid particles in a hydraulic cyclone, Chemical Engineering Research and Design, Volume 30, p.87-108 (1952)

[5] Wills B.A., Napier-Munn T.: Wills' mineral processing technology, 7. Edition, Elsevier Ltd., Oxford, p.203-223 (2006)

[6] Gerla J.H.: Modelling, measurement and manipulation of crystallizers: the role of classifiers and hydrodynamics, Doctoral thesis, Delft University of Technology (1995)

[7] van Ommen R.: Optimization of classification results by controlling of hydrocyclone process parameters, Dissertation, Montanuniversitaet Leoben (2011)

[8] Hacifazlioglu H.: Application of the modified water-only cyclone for cleaning fine coals in a Turkish washery, and comparison of its performance results with those of spiral and flotation, Fuel Processing Technology, Volume 102, p.11-17 (2012)

[9] Schmidt M.P, Turner P.A.: Flat bottom or horizontal cyclones – which is the right for you?, World Mining Equipment, p.151-152 (1993)

[10] Fuerstenau M.C., Kenneth N.H.: Principles of mineral processing, Society for Mining, Metallurgy and Exploaration Inc., Colorado, p.156-168 (2003)

[11] Ghodrat M. et al: Numerical analysis of hydrocyclones with different vortex finder configurations, Minerals Engineering, Volume 63, p.125-138 (2014)

[12] Wang B., Yu A.B.: Numerical study of particle–fluid flow in hydrocyclones with different body dimensions, Minerals Engineering, Volume 19, p.1022-1033 (2006)

[13] Lynch A.J., Rao T.C. et al: The influence of hydrocyclone diameter on reduced-efficiency curves, International Journal of Mineral Processing, Volume 1, p.173-181 (1974)

[14] http://www.flsmidth.com/~/media/PDF%20Files/Krebs/04-204FLSKrebs_gMAX_brochure_email.ashx (Accessed 22 May 2016)

SYMBOLS

A	area [m²]
a_r	radial acceleration [m/s²]
D	diameter [mm]
D50	cut size, the particle size for which 50% of the particles in the feed report to the underflow [µm]
d	particle size diameter [µm]
E_{UF}	recovery of underflow [%]
$E_{UF,corr}$	corrected recovery of underflow [%]
m_l	mass of liquid [g]
m_s	mass of solid [g]
$m_{\mu j}$	mass content of characteristics class µ in product j [%]
$m_{\mu 0}$	mass content of characteristics class µ in feed [%]
η	dynamic viscosity [mPa·s]
Δp	pressure drop [psi]
RSU	right side up
r	radius [mm]
r_{mj}	mass yield of product j [%]
$\rho_{s,l,p}$	specific gravity of solid, liquid, pulp [g/cm³]
$T_{\mu j}$	partition number of characteristics class µ according to product j [%]
$T_{\alpha(D)}$	partition number of a specific particle fraction D [%]
USD	upside down
VF	vortex finder
v_t	tangential velocity [m/s]
v_s	terminal settling velocity [m/s]
WOC	water-only cyclone
$y_{UF,i}$	actual mass fraction of a particle size reporting to underflow [%]
$y_{UF,i,corr}$	corrected mass fraction of a particle size reporting to underflow [%]

LIST OF FIGURES

LIST OF TABLES

APPENDIX

KREBS CYCLONE PROBLEM ANALYSIS

SHEET 1
DATE 10/9/15
BY LH

5505 West Gillette Road, Tucson, AZ 85743
TEL: (520) 744-8200 FAX: (520) 744-8300

CLIENT: Krebs
PROBLEM: Compare Flat Bottom & Water Only & 20^0

NUMBER, MODEL OF CYCLONE: gMAX10-20

	INLET	VORTEX FINDER	APEX	PRESSURE
ORIFICES:	8,4 in²	4,00 in.	1,75 in.	5 PSI

SPEC. GRAVITY: SOLIDS 2,80 LIQUID 1,00

	FEED	OVERFLOW	UNDERFLOW	WATER-SPLIT
STPH SOLIDS	31,9	21,6	10,3	17,8
STPH LIQUID	29,6	24,4	5,3	
STPH PULP	61,5	46,0	15,6	
% SOLIDS WT	51,8	47,0	66,1	
S.G. PULP	1,5	1,4	1,7	
% SOLIDS VOL	27,8	24,1	41,1	
U.S. GPM PULP	164,1	128,3	35,8	
cyclone.wk4 Ver 4.1		% CIRCULATING LOAD	47,7	

Ref # 289/35.5/3.95/0.9972 Ref. File: FlatBottom

MICRON	FEED			OVERFLOW			UNDERFLOW			ACT	CORR
	CUM % +	IND % +	STPH	CUM % +	IND % +	STPH	CUM % +	IND % +	STPH	REC	REC
850	8,47	8,47	2,703	0,002	0,002	0,000	26,25	26,25	2,703	100,0	100,0
600	10,48	2,01	0,64	0,080	0,078	0,017	32,29	6,05	0,62	97,4	96,8
425	13,44	2,96	0,94	0,681	0,601	0,130	40,19	7,90	0,81	86,2	83,3
300	16,92	3,49	1,11	2,555	1,874	0,405	47,06	6,87	0,71	63,6	55,7
212	21,51	4,59	1,46	6,584	4,029	0,870	52,83	5,77	0,59	40,6	27,7
150	29,67	8,15	2,60	15,507	8,923	1,927	59,37	6,54	0,67	25,9	9,9
106	44,96	15,29	4,88	33,649	18,142	3,919	68,69	9,32	0,96	19,7	2,3
75	56,23	11,27	3,60	47,145	13,496	2,915	75,29	6,60	0,68	18,9	1,4
53	64,41	8,18	2,61	57,06	9,916	2,142	79,84	4,55	0,47	17,9	0,2
45	67,45	3,04	0,97	60,71	3,65	0,789	81,59	1,75	0,18	18,6	1,0
38	69,86	2,41	0,77	63,61	2,90	0,626	82,97	1,38	0,14	18,4	0,8
-38	100,00	30,14	9,61	100,00	36,39	7,86	100,00	17,03	1,75	18,2	0,6
TOTAL		100,00	31,90		100,00	21,60		100,00	10,30	32,3	17,6

Figure 36: Calculation sheet

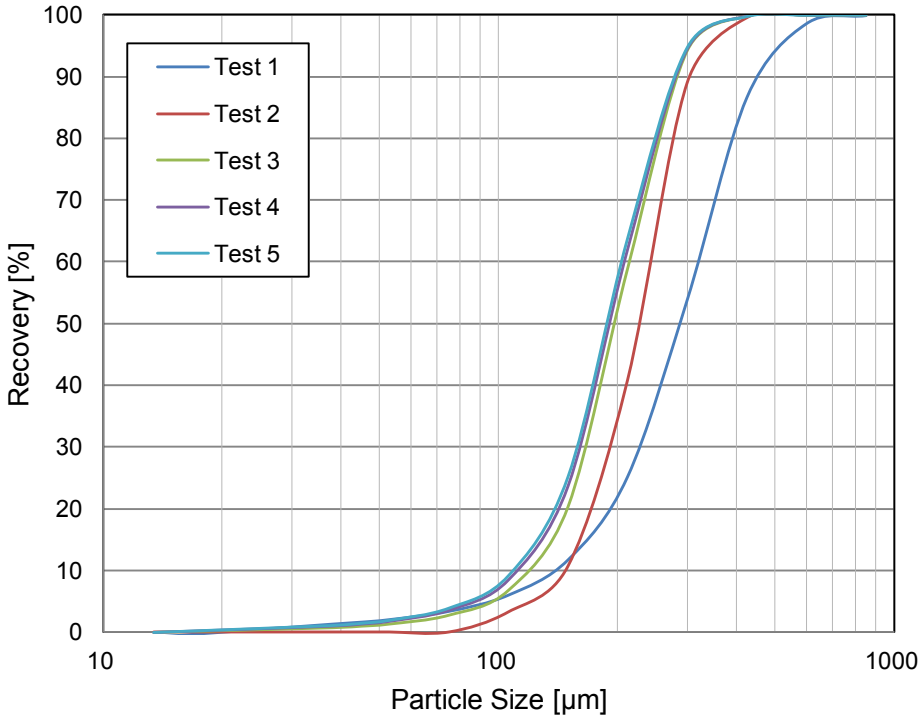

Figure 37: Partition curves of tests with the standard cyclone with VF diameter of 4 inch, VF standard length, apex diameter of 1.5 inch and apex installation right side up at 5,10,15,20 and 25 psi pressure drop.

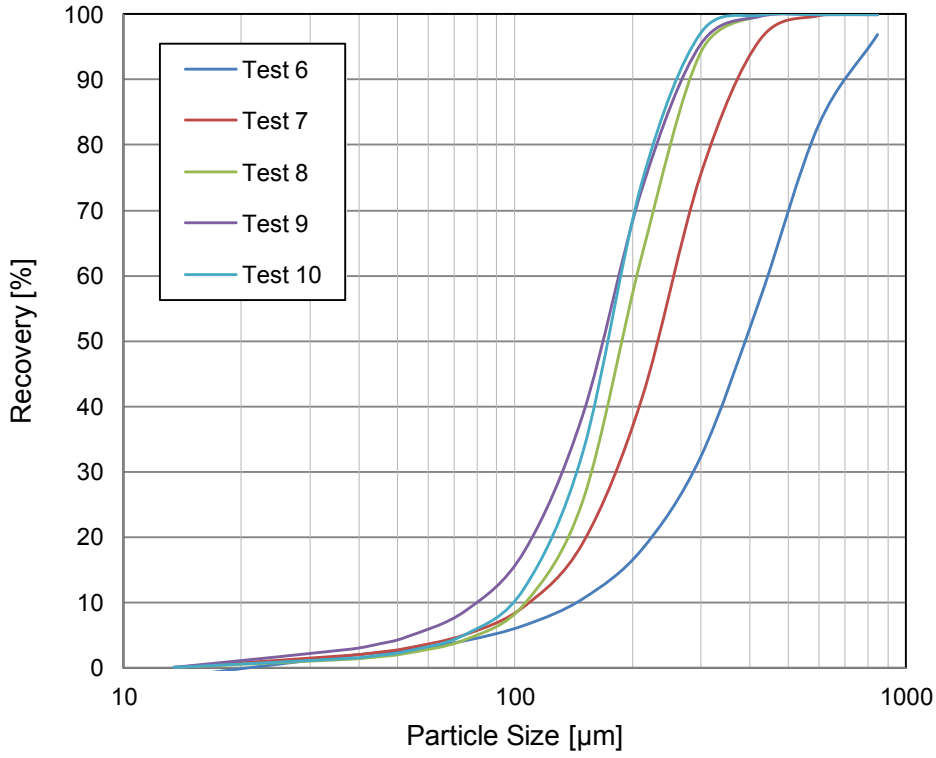

Figure 38: Partition curves of tests with the standard cyclone with VF diameter of 3 inch, VF standard length, apex diameter of 1.5 inch and apex installation right side up at 5,10,15,20 and 25 psi pressure drop.

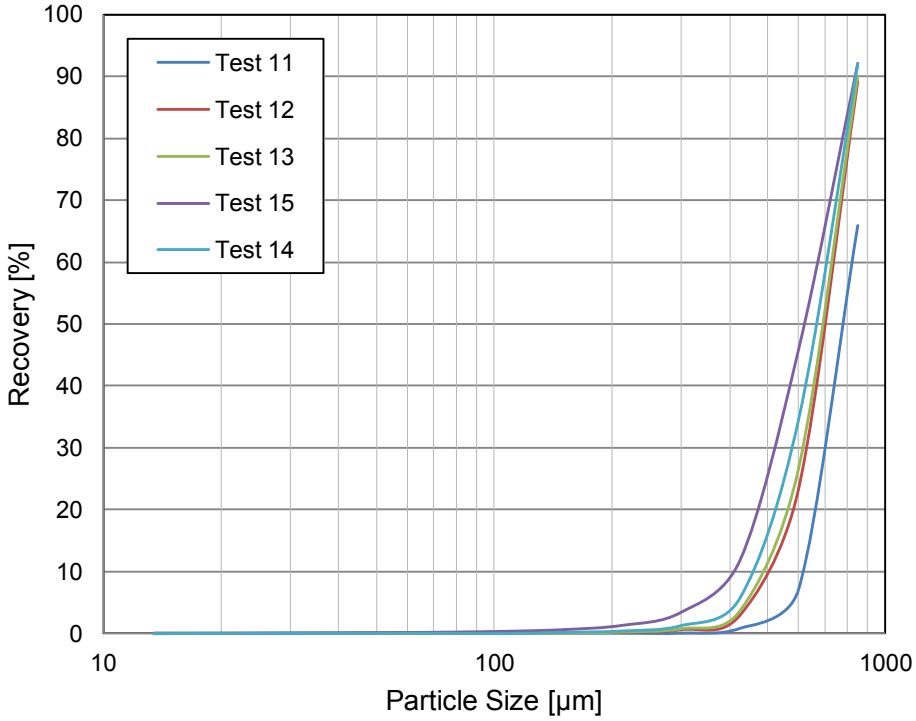

Figure 39: Partition curves of tests with the WOC with VF diameter of 4 inch, VF standard length, apex diameter of 1.5 inch and apex installation upside down at 5,10,15,20 and 25 psi pressure drop.

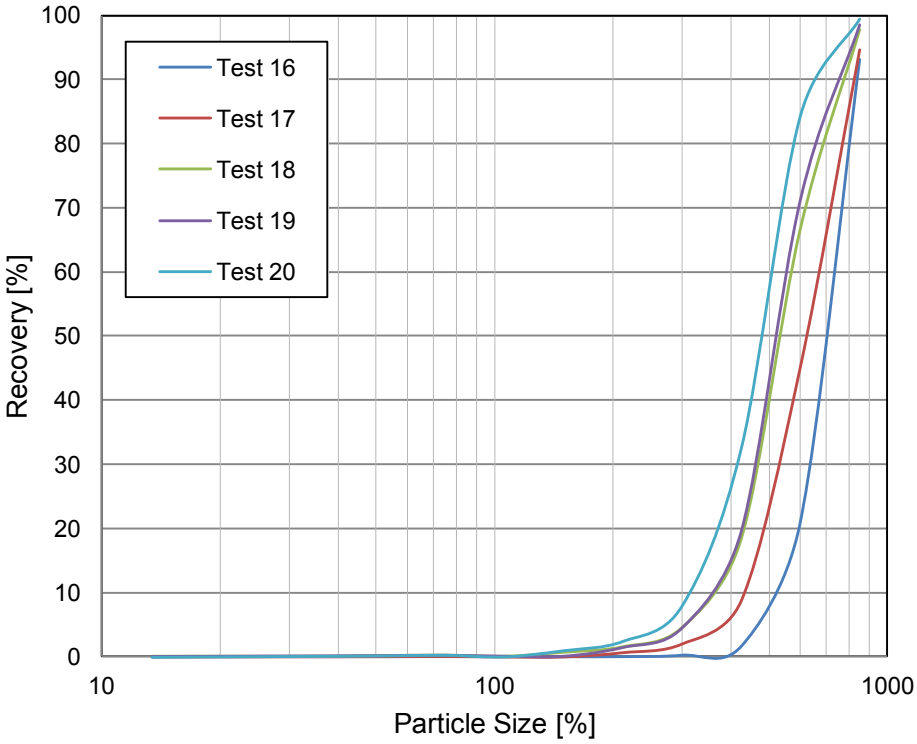

Figure 40: Partition curves of tests with the WOC with VF diameter of 3 inch, VF standard length, apex diameter of 1.5 inch and apex installation upside down at 5,10,15,20 and 25 psi pressure drop.

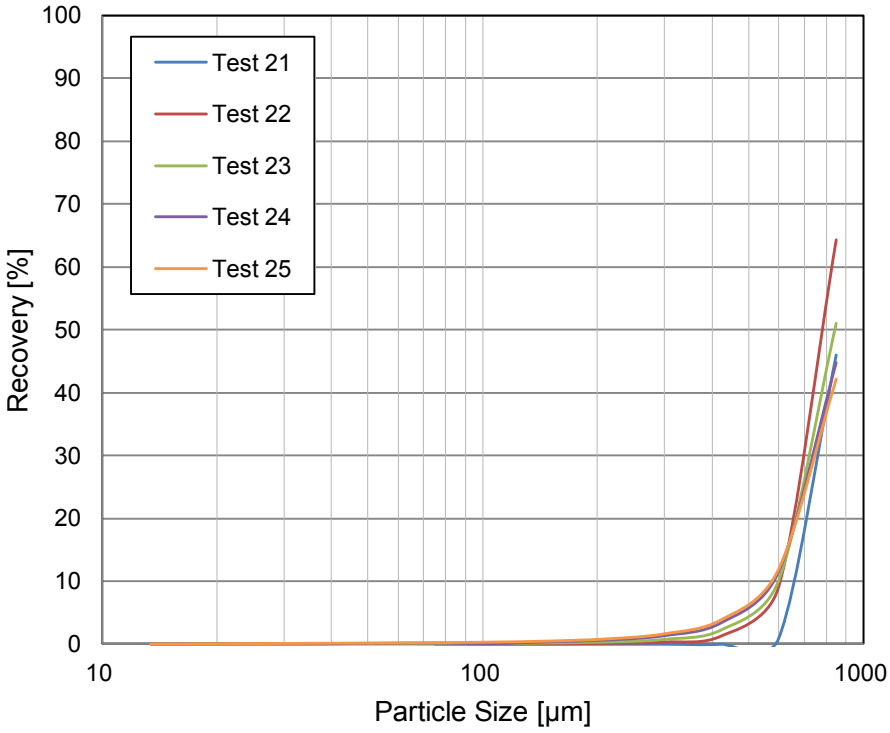

Figure 41: Partition curves of tests with the WOC with VF diameter of 4 inch, VF long length, apex diameter of 1.5 inch and apex installation upside down at 5,10,15,20 and 25 psi pressure drop.

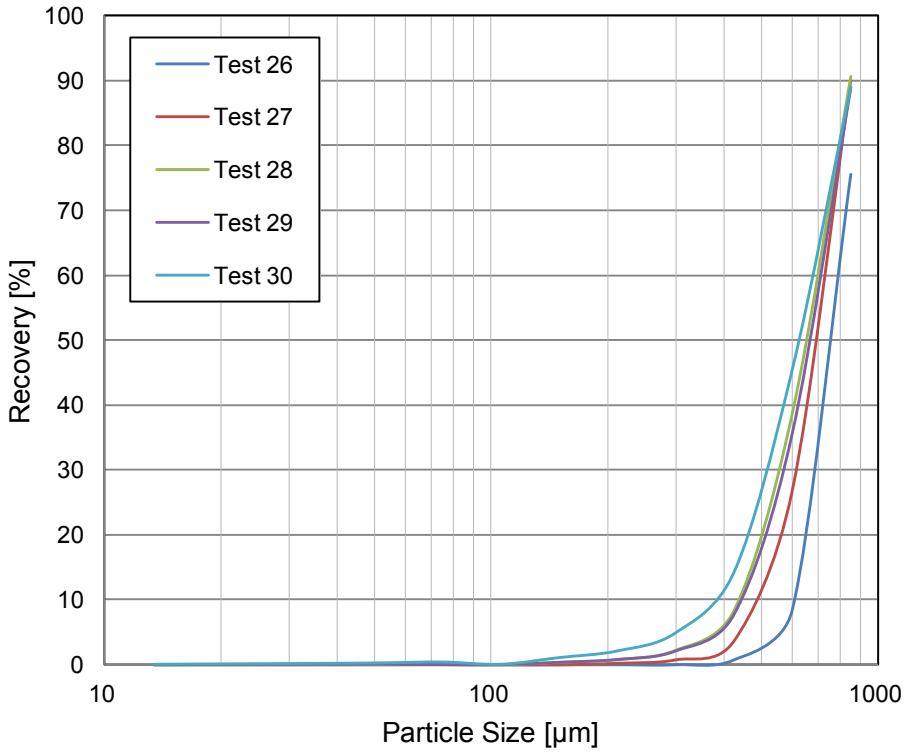

Figure 42: Partition curves of tests with the WOC with VF diameter of 3 inch, VF long length, apex diameter of 1.5 inch and apex installation upside down at 5,10,15,20 and 25 psi pressure drop.

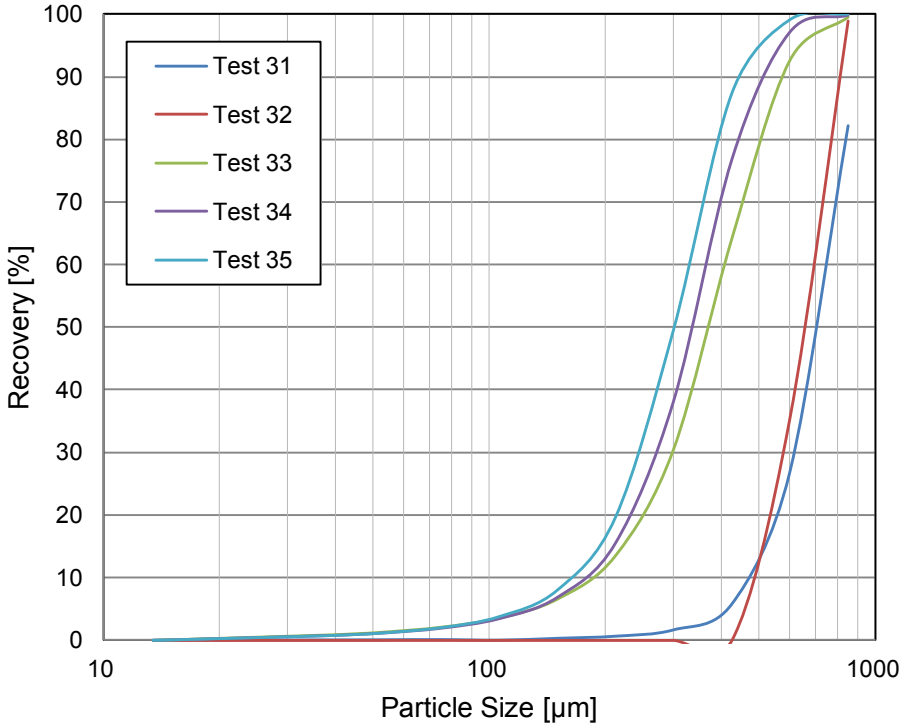

Figure 43: Partition curves of tests with the flat bottom cyclone with VF diameter of 3 inch, VF standard length, apex diameter of 1.5 inch and apex installation right side up at 5,10,15,20 and 25 psi pressure drop.

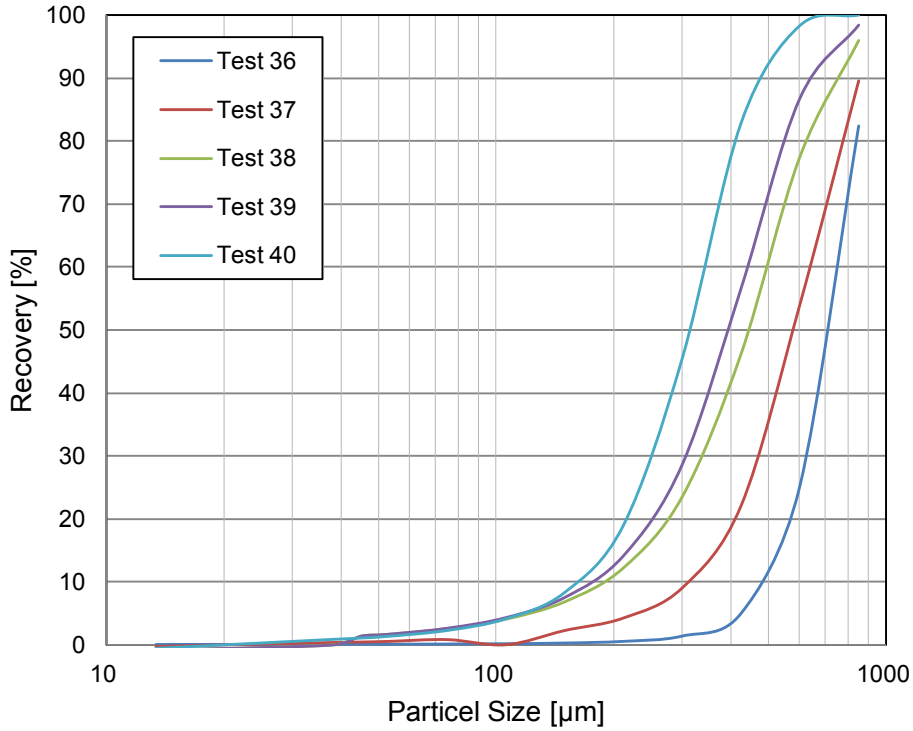

Figure 44: Partition curves of tests with the flat bottom cyclone with VF diameter of 4 inch, VF long length, apex diameter of 1.5 inch and apex installation right side up at 5,10,15,20 and 25 psi pressure drop.

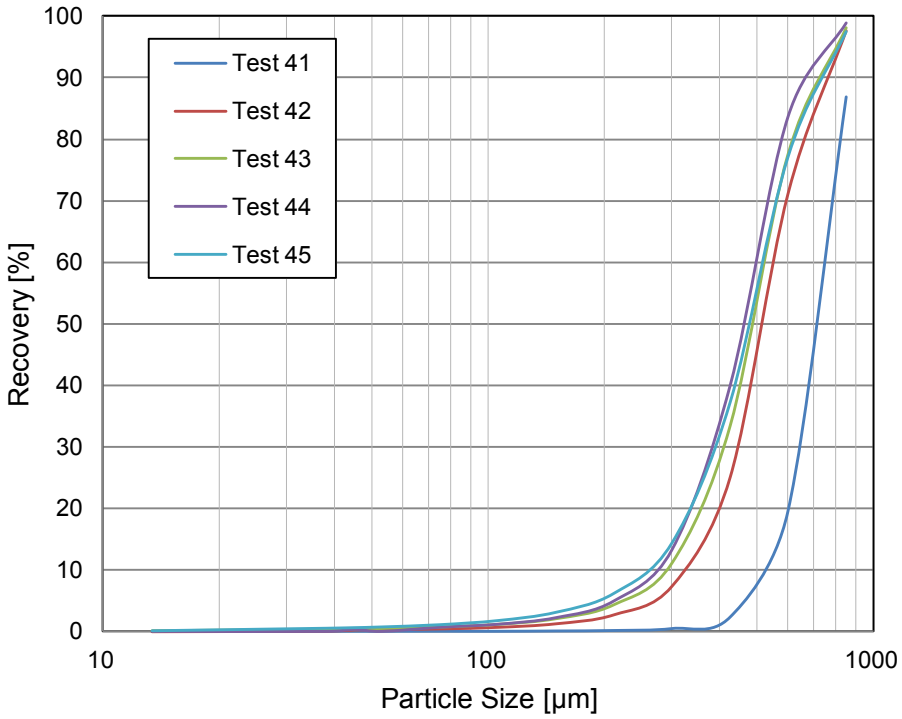

Figure 45: Partition curves of tests with the flat bottom cyclone with VF diameter of 4 inch, VF long length, apex diameter of 1.5 inch and apex installation right side up at 5,10,15,20 and 25 psi pressure drop.

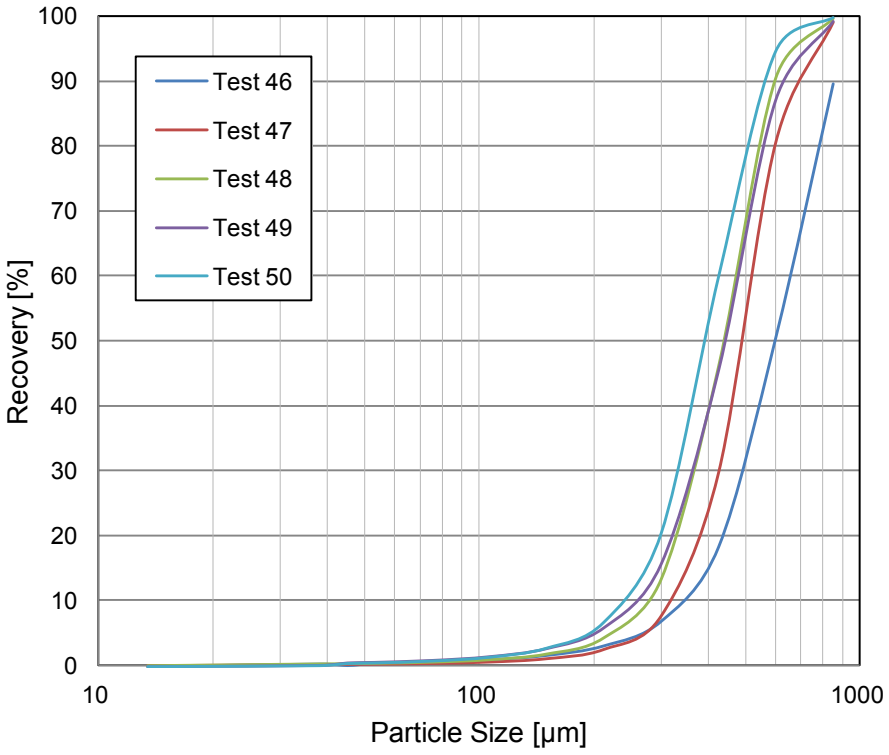

Figure 46: Partition curves of tests with the flat bottom cyclone with VF diameter of 4 inch, VF standard length, apex diameter of 1.5 inch and apex installation right side up at 5,10,15,20 and 25 psi pressure drop.

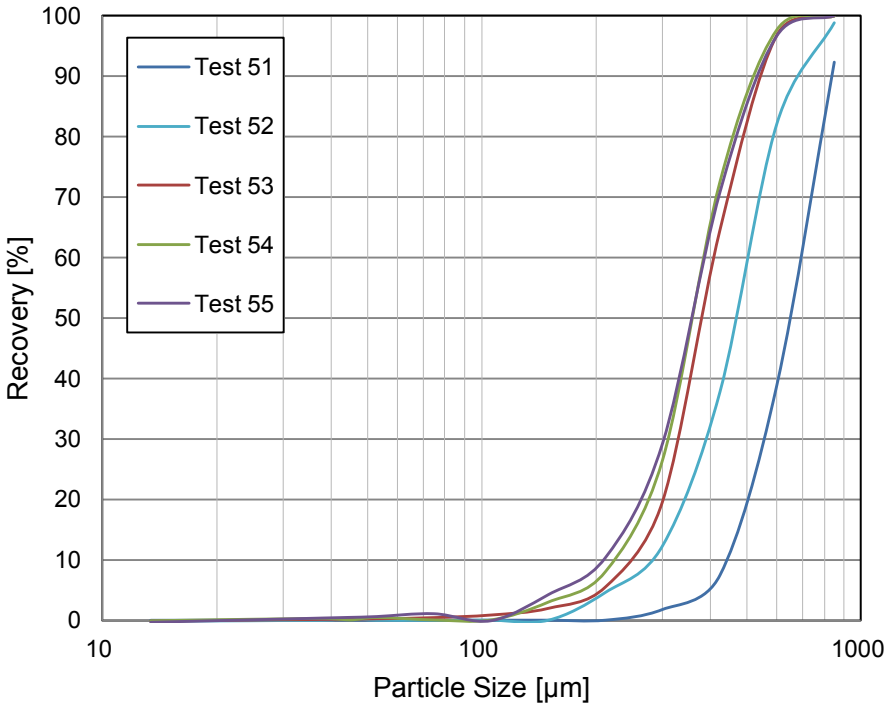

Figure 47: Partition curves of tests with the flat bottom cyclone with VF diameter of 4 inch, VF standard length, apex diameter of 2.5 inch and apex installation right side up at 5,10,15,20 and 25 psi pressure drop.

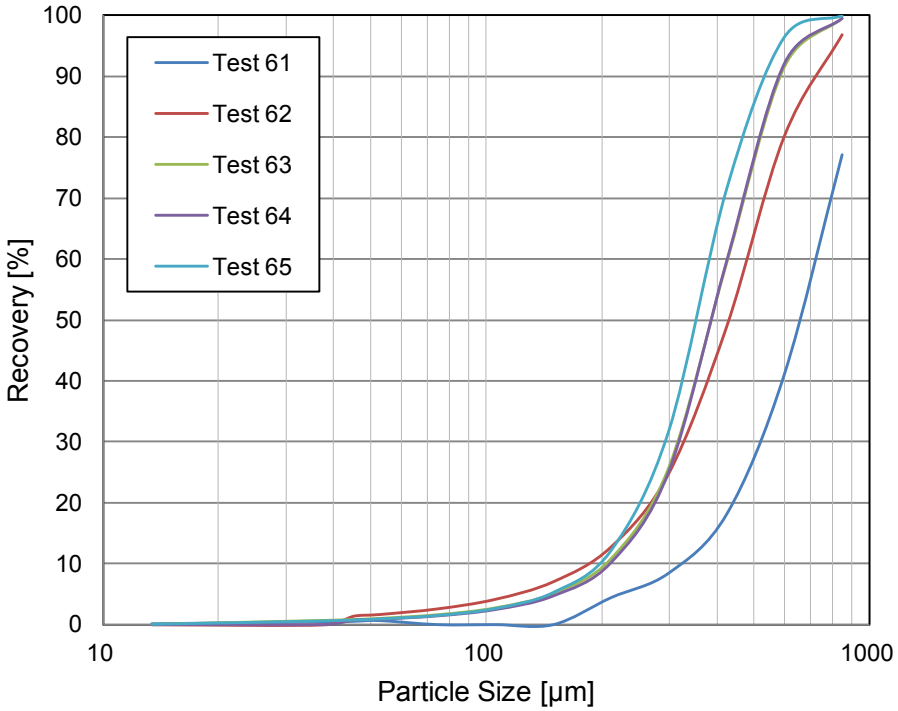

Figure 48: Partition curves of tests with the WOC cyclone with VF diameter of 4 inch, VF long length, apex diameter of 1.5 inch and apex installation right side up at 5,10,15,20 and 25 psi pressure drop.

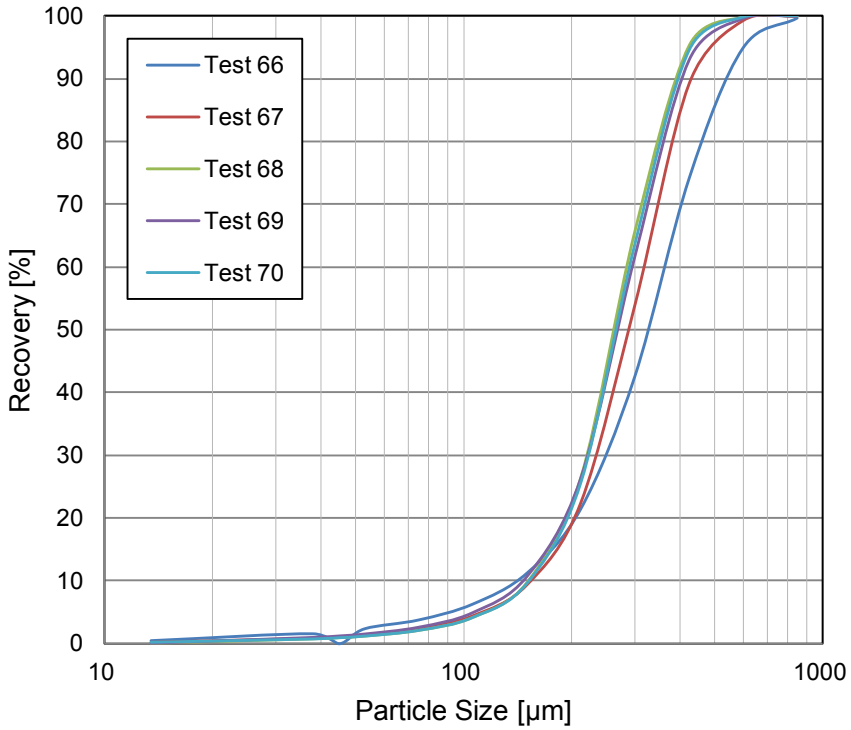

Figure 49: Partition curves of tests with the WOC cyclone with VF diameter of 4inch, VF standard length, apex diameter of 1.5 inch and apex installation right side up at 5,10,15,20 and 25 psi pressure drop

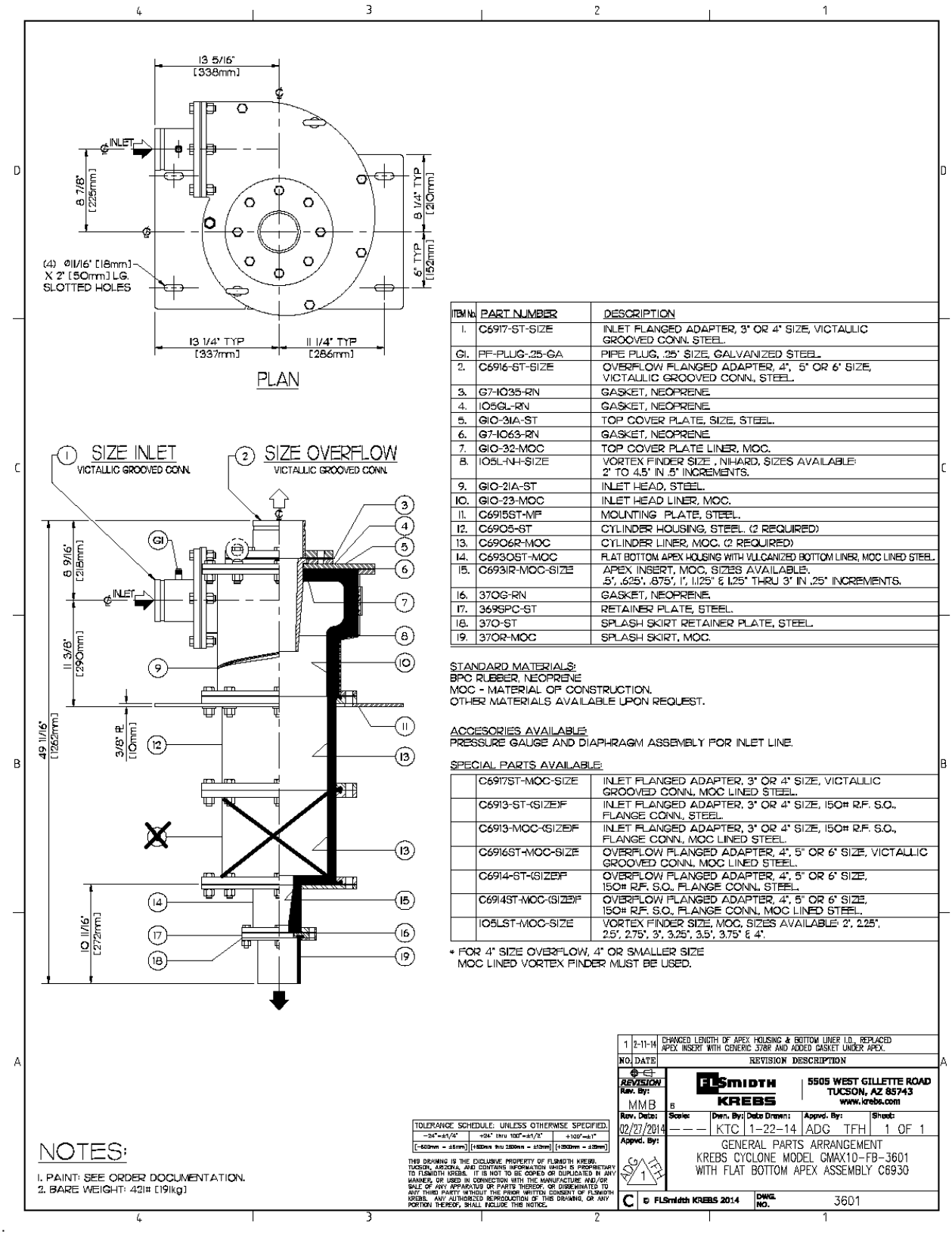

ITEM No.	PART NUMBER	DESCRIPTION
1.	C6917-ST-SIZE	INLET FLANGED ADAPTER, 3" OR 4" SIZE, VICTAULIC GROOVED CONN. STEEL.
GI.	PF-PLUG-.25-GA	PIPE PLUG, .25" SIZE, GALVANIZED STEEL.
2.	C6916-ST-SIZE	OVERFLOW FLANGED ADAPTER, 4", 5" OR 6" SIZE, VICTAULIC GROOVED CONN., STEEL.
3.	G7-1035-RN	GASKET, NEOPRENE.
4.	105GL-RN	GASKET, NEOPRENE.
5.	G10-31A-ST	TOP COVER PLATE, SIZE, STEEL.
6.	G7-1063-RN	GASKET, NEOPRENE.
7.	G10-32-MOC	TOP COVER PLATE LINER, MOC.
8.	105L-NH-SIZE	VORTEX FINDER SIZE , NIHARD, SIZES AVAILABLE: 2" TO 4.5" IN .5" INCREMENTS.
9.	G10-21A-ST	INLET HEAD, STEEL.
10.	G10-23-MOC	INLET HEAD LINER, MOC.
11.	C6915ST-MP	MOUNTING PLATE, STEEL.
12.	C6905-ST	CYLINDER HOUSING, STEEL. (2 REQUIRED)
13.	C6906R-MOC	CYLINDER LINER, MOC. (2 REQUIRED)
14.	C6930ST-MOC	FLAT BOTTOM APEX HOUSING WITH VULCANIZED BOTTOM LINER, MOC LINED STEEL.
15.	C6931R-MOC-SIZE	APEX INSERT, MOC, SIZES AVAILABLE: .5", .625", .875", 1", 1.125" & 1.25" THRU 3" IN .25" INCREMENTS.
16.	370G-RN	GASKET, NEOPRENE.
17.	369SPC-ST	RETAINER PLATE, STEEL.
18.	370-ST	SPLASH SKIRT RETAINER PLATE, STEEL.
19.	370R-MOC	SPLASH SKIRT, MOC.

STANDARD MATERIALS:
BPC RUBBER, NEOPRENE
MOC - MATERIAL OF CONSTRUCTION.
OTHER MATERIALS AVAILABLE UPON REQUEST.

ACCESORIES AVAILABLE:
PRESSURE GAUGE AND DIAPHRAGM ASSEMBLY FOR INLET LINE.

SPECIAL PARTS AVAILABLE:

	C6917ST-MOC-SIZE	INLET FLANGED ADAPTER, 3" OR 4" SIZE, VICTAULIC GROOVED CONN, MOC LINED STEEL.
	C6913-ST-(SIZE)F	INLET FLANGED ADAPTER, 3" OR 4" SIZE, 150# R.F. S.O., FLANGE CONN., STEEL.
	C6913-MOC-(SIZE)F	INLET FLANGED ADAPTER, 3" OR 4" SIZE, 150# R.F. S.O., FLANGE CONN., MOC LINED STEEL.
	C6916ST-MOC-SIZE	OVERFLOW FLANGED ADAPTER, 4", 5" OR 6" SIZE, VICTAULIC GROOVED CONN, MOC LINED STEEL.
	C6914-ST-(SIZE)F	OVERFLOW FLANGED ADAPTER, 4", 5" OR 6" SIZE, 150# R.F. S.O., FLANGE CONN., STEEL.
	C6914ST-MOC-(SIZE)F	OVERFLOW FLANGED ADAPTER, 4", 5" OR 6" SIZE, 150# R.F. S.O., FLANGE CONN., MOC LINED STEEL.
	105LST-MOC-SIZE	VORTEX FINDER SIZE, MOC, SIZES AVAILABLE: 2", 2.25", 2.5", 2.75", 3", 3.25", 3.5", 3.75" & 4".

* FOR 4" SIZE OVERFLOW, 4" OR SMALLER SIZE MOC LINED VORTEX FINDER MUST BE USED.

NO.	DATE	REVISION DESCRIPTION
1	2-11-14	CHANGED LENGTH OF APEX HOUSING & BOTTOM LINER I.D., REPLACED APEX INSERT WITH GENERIC 378R AND ADDED GASKET UNDER APEX.

REVISION Rev. By: MMB | Rev. Date: 02/27/2014 | Appvd. By:

FLSmidth KREBS
5505 WEST GILLETTE ROAD
TUCSON, AZ 85743
www.krebs.com

Scale:	Dwn. By:	Date Drawn:	Appvd. By:	Sheet:
— — —	KTC	1-22-14	ADG TFH	1 OF 1

GENERAL PARTS ARRANGEMENT
KREBS CYCLONE MODEL GMAX10-FB-3601
WITH FLAT BOTTOM APEX ASSEMBLY C6930

C © FLSmidth KREBS 2014 DWG. NO. 3601

Figure 50: Technical drawing of flat bottom hydrocyclone

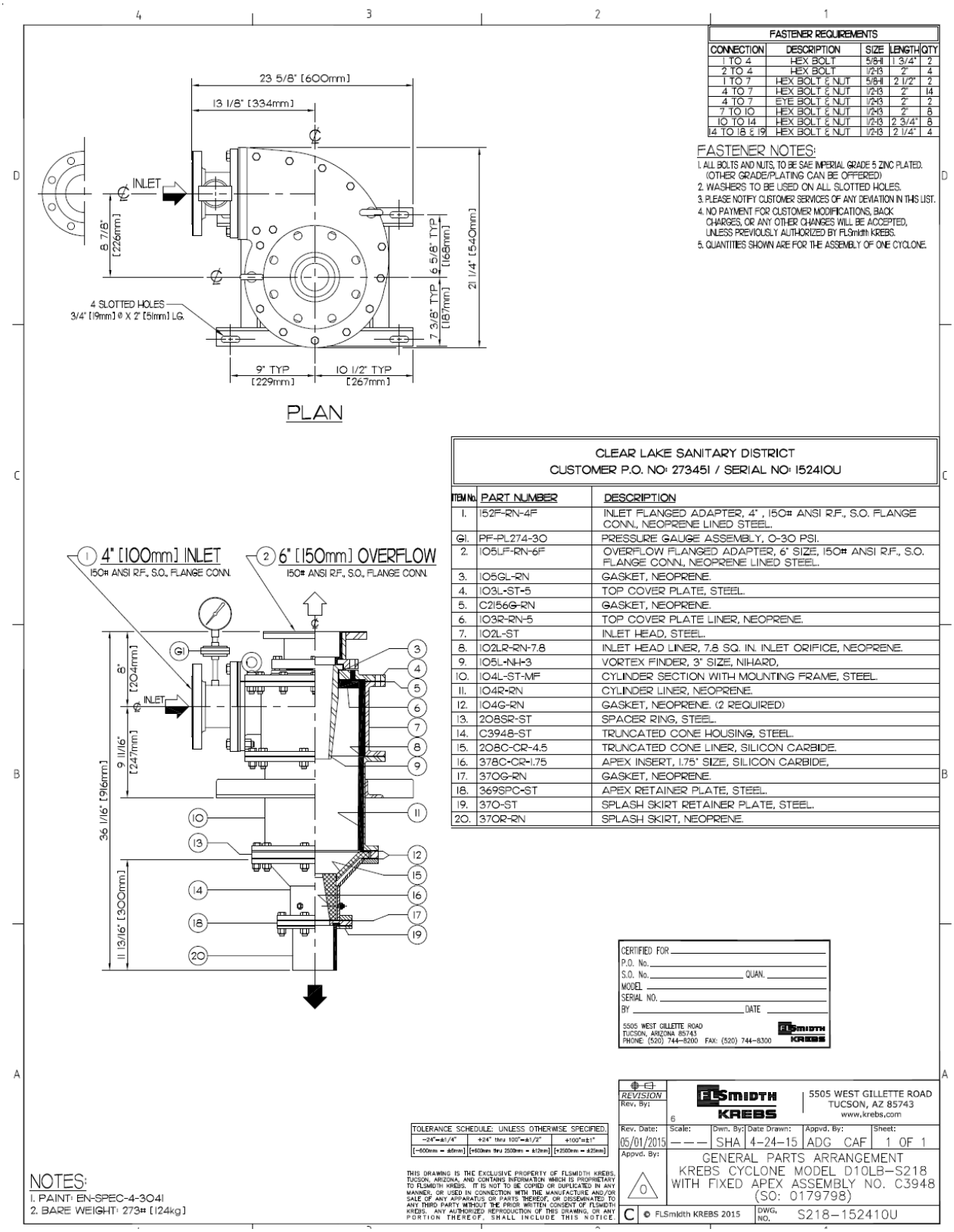

Figure 51: Technical drawing of water-only cyclone

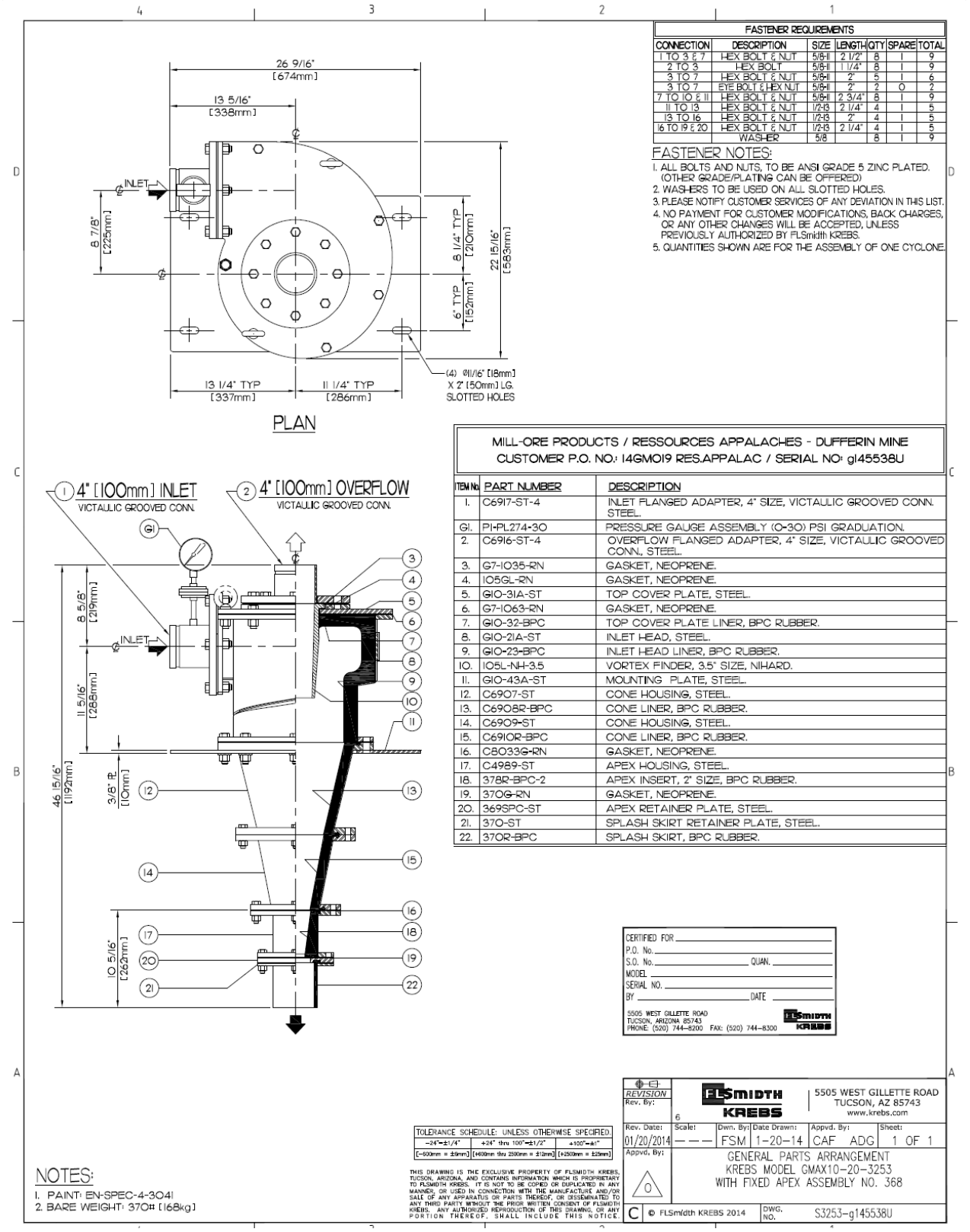

Figure 52: Technical drawing of standard hydrocyclone

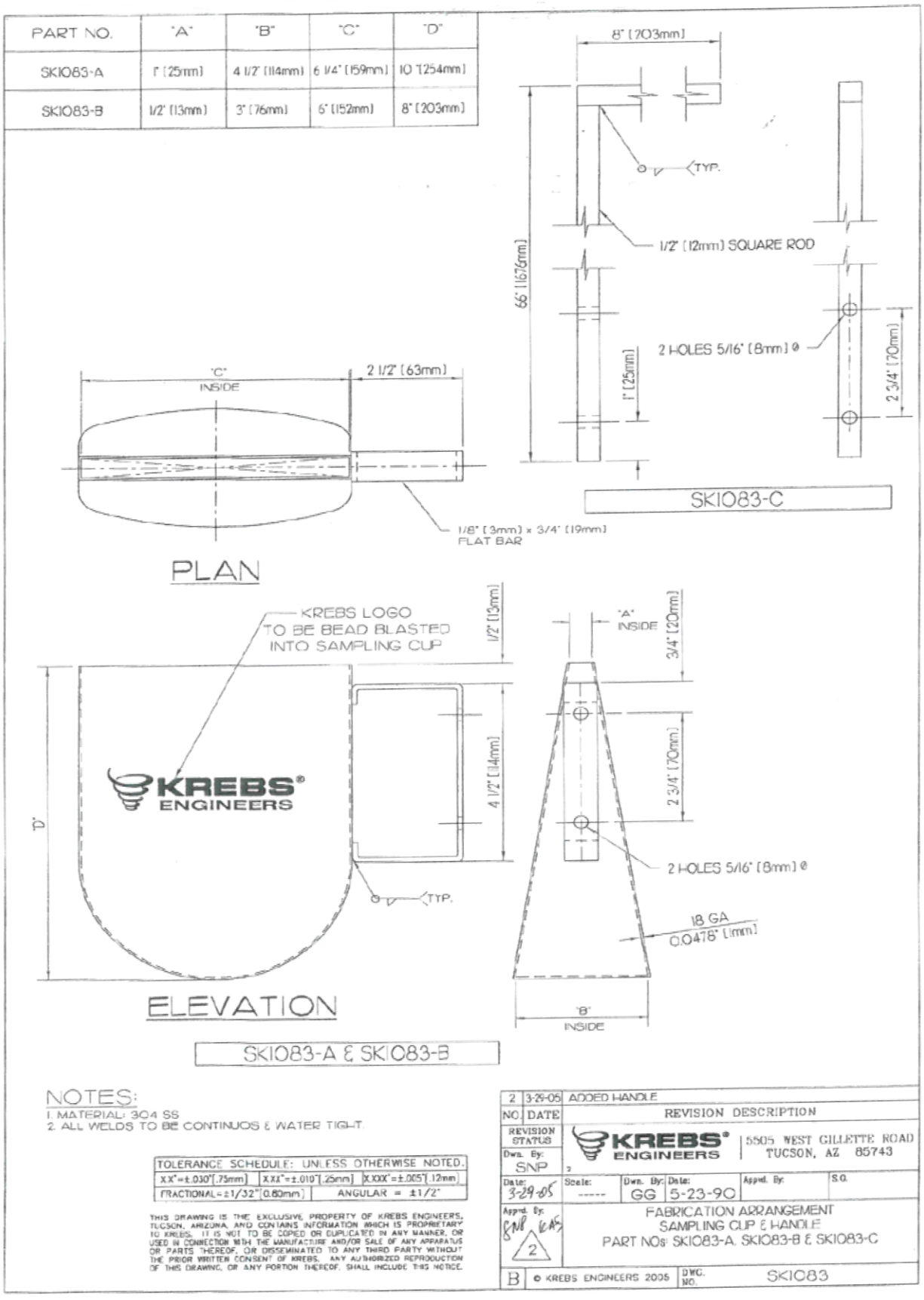

Figure 53: Technical drawing of the sample cutter